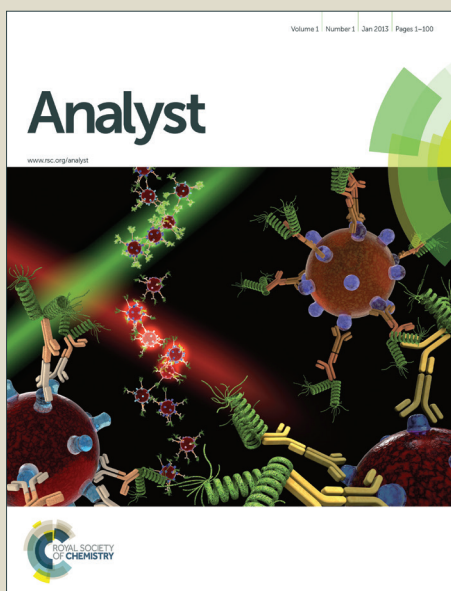


Analyst

Accepted Manuscript



This is an *Accepted Manuscript*, which has been through the Royal Society of Chemistry peer review process and has been accepted for publication.

Accepted Manuscripts are published online shortly after acceptance, before technical editing, formatting and proof reading. Using this free service, authors can make their results available to the community, in citable form, before we publish the edited article. We will replace this *Accepted Manuscript* with the edited and formatted *Advance Article* as soon as it is available.

You can find more information about *Accepted Manuscripts* in the [Information for Authors](#).

Please note that technical editing may introduce minor changes to the text and/or graphics, which may alter content. The journal's standard [Terms & Conditions](#) and the [Ethical guidelines](#) still apply. In no event shall the Royal Society of Chemistry be held responsible for any errors or omissions in this *Accepted Manuscript* or any consequences arising from the use of any information it contains.

Nanomaterial-based Biosensors using Dual Transducing Elements for Solution Phase Detection

Cite this: DOI: 10.1039/x0xx00000x

Ning Li^a, Xiaodi Su^{a*}, Yi Lu^{a,b*}

Received 00th January 2012,
Accepted 00th January 2012

DOI: 10.1039/x0xx00000x

www.rsc.org/

Biosensors incorporating nanomaterials have demonstrated superior performance compared to their conventional counterparts. Most reported sensors use nanomaterials as a single transducer of signals, while biosensor designs using dual transducing elements have emerged as new approaches to further improve the overall sensing performance. This review focuses on recent development of nanomaterial-based biosensors using dual transducing elements for solution phase detection. The review is organized by a brief introduction of the commonly used nanomaterial transducers suitable for designing the dual elements sensors, including quantum dots, metal nanoparticles, upconversion nanoparticles, graphene, graphene oxide, carbon nanotube, and carbon nanodots. It is followed by the presentation of four basic design principles, namely Förster Resonance Energy Transfer (FRET), Amplified Fluorescence Polarization (AFP), Bio-barcode Assay (BCA) and Chemiluminescence (CL), involving either two kinds of nanomaterials, or one nanomaterial and an organic luminescent agent (e.g. organic dyes, luminescent polymers) as dual transducers. Biomolecular and chemical analytes or biological interactions are detected by their control of the assembly and disassembly of the two transducing elements that will change the distance between them, the size of fluorophore-containing composite, or the catalytic properties of the nanomaterial transducers, among other property changes. Comparative discussions on their respective design rules and overall performances are presented afterwards. Compared with the single transducer biosensor design, such dual-transducer configuration exhibits much enhanced flexibility and design versatility, allowing biosensors to be more specifically devised for various purposes. The review is ended by highlighting some of the further development opportunities in this field.

Introduction

Detection of biological agents and sensing of particular bio-reactions are of great importance for biochemical and biomedical applications,¹ especially for early diagnosis of certain diseases, monitoring therapeutic prognosis and critical biomarker identification. While various types of bioassay methods that are available, many are costly, labour intensive and involving tedious assaying steps. Thus, significant demands are still not met, particularly on developing biosensors with high selectivity and sensitivity, as well as reasonable robustness, cost-effectiveness, versatility and portability.² A typical biosensor features two basic components: a biological sensing probe that provides selective target binding and a transducing element that transforms the binding into detectable signals. Therefore, the performance of a biosensor, in terms of limit of detection (LOD), selectivity, response time and signal-to-noise ratio, depends heavily on the quality of biological sensing probes and transducing elements, as well as the interfaces between them. This requirement imposes major effort on the development of related materials.

In 1959, Richard Feynman pointed out that “There’s plenty of room at the bottom.” Decades later, nanoscale science and

engineering emerges and exerts extraordinary impact on many technological fields. Owing to the quantum confinement effect induced by its 10^{-9} m scale, nanomaterials demonstrate various unprecedented and unique properties that can be applied broadly in improving the target-recognizing and signal-transducing mechanisms in biosensor design.³ In addition, they have comparable size with the common biomolecules such as DNA and proteins, affording integration of the nanomaterials with biomolecules for advanced biosensor development.⁴⁻⁶ Up to date, a large number of nanomaterials-based biosensors have been reported and reviewed from different perspectives, such as targets to be detected, type of transducing elements, detection principles, sensing performance.^{5,7-29} Among all the reported works, however, many of them use a single nanomaterial sensing element to generate signals, such as the colour change of metal nanoparticles due to analyte-induced aggregation and dispersion,^{8,10,15,20,23} or the conductance change in 1-D nanowire (e.g., carbon nanotube or conducting polymer chain) induced by analyte adsorption.²⁹

In addition to the biosensors involving a single nanomaterial transducer, biosensors using dual transducing elements of inorganic nanomaterials or combination of an inorganic nanomaterial with organic luminescent agent offer greater

promise of advancing the biosensor research by enhancing both the sensitivity and selectivity of the sensors.^{9-11,15,19,20,23} However, few specific review articles have focused and systematically covered this topic. We hereby provide a review focusing on the solution-phase biosensors with dual transducing elements, particular on selection of transducing materials, design principle, application and performance. The dual transducing elements here are exclusive of the sensing probes that are often biomolecules. Benefit from the dual transducers and their interplay with the sensing probe, we can therefore expect improved assay sensitivity and selectivity over single transducer design. Herein, the term “biosensor” is referred to any assay method that can detect certain biological/biochemical substances or monitor biological reactions/mechanism, with the use of one or more physicochemical transducer(s), although in some other studies stricter criteria apply (e.g., capable of continuously sensing a biological process or target³⁰). “Solution-phase” bioassay/biosensor sometimes is also called “Mix-and-Measure” or “Separation-Free” detection method, in which both target binding and signal transducing occur in homogeneous solution, and the signal acquisition can be accomplished using common spectrophotometers and/or microplate readers, but not sophisticated equipment.

Within this review, we will firstly introduce several important classes of nanomaterials, especially their unique chemical and optical properties appealing to biosensor construction. Then, the majority of the discussion will focus on the various dual-transducer-based mechanisms including Förster Resonance Energy Transfer (FRET), Amplified Fluorescence Polarization (AFP), Bio-barcode Assay (BCA) and Chemiluminescence (CL), as well as their representative examples that have been demonstrated by worldwide research communities recently. Due to the availability of the large variety of fluorescent transducers and labels, FRET, which describes the coupling energy transfer between two fluorescent agents, is highly versatile, thus accounts for considerably larger quantity of literature than the other three. We therefore divide its discussion based on the target analytes (e.g., metal ions and small molecules, DNA, proteins and enzymes). Schematic drawings are created in the FRET and AFP sections, to provide visualization of the design rules for different analytes under respective principle. With the wide coverage of inorganic nanomaterials, ranging from quantum dots, metal nanoparticles, upconversion nanoparticles, and carbon based nanomaterials (e.g., graphene, graphene oxide, carbon nanotube, and carbon dots), this review provides a perspective of the emerging of different generation of nanomaterials for analytical usage in the fields of chemical sensing, biosensing and diagnosis. At the end of this review, we also try to answer the following reflective questions: What are the additional opportunities that nanomaterials-based dual-transducer biosensors can provide in comparison to the single transducer-based counterpart? And what are the advantages and disadvantages for each of the four dual-transducer sensing principles discussed in this review? (supported by a Holland Vocational Interest Test illustration)

Nanomaterials used for Constructing Biosensors

The unique chemical and physical properties of utilized nanomaterials, as well as their interaction with sensing probes and the other transducing elements, lay the foundation for biosensor construction and excellent performances. In this section, we aim to provide a brief introduction on several nanomaterials that have been intensively investigated for

constructing dual-transducer based biosensors. The covered materials include quantum dots (QDs), metal nanoparticles (mNPs), upconversion nanoparticles (UCNPs), graphene oxide (GO), carbon nanotubes (CNTs), as well as carbon nanodots (CDs). Table 1 illustrates the favourable properties, major roles of each nanomaterial in dual-transducer based biosensors, as well as the challenges that need to be taken care of for sensor design.

Quantum Dots

Quantum dots (QDs), firstly reported by Brus and colleagues in 1983,³¹ is a family of semiconducting nanocrystallized fluorophore that is small enough to exhibit the quantum confinement effect (

Figure 1 a and b).¹³ They have been widely explored in diverse biological fields primarily as fluorescent labelling agents, by virtue of their excellent brightness and photostability. Many reviews have been published regarding their physical properties, synthesis, surface chemistry, and various applications such as biosensors, clinical therapy and *in vivo* bioimaging.^{13,21,22,32-35} Of particular interests are their broad absorbance spectrum, narrow emission band and tunable emission wavelength, which afford high flexibility in choosing the excitation wavelength and modulating the emission spectra among different QDs (

Figure 1 c). These optical properties are intrinsically favourable for designing biosensors with dual transducing elements. For example, coupling QDs into the FRET system is an effective approach to improve design versatility and performances, by virtue of the QDs compatibility with various other fluorophores and quenchers.³⁶ In addition, QDs have multitude functionalization sites on their large surface area. This becomes advantageous when conjugation of several sensing probes is desired for the multiplexed detection³⁷ or for improving the detection sensitivity with multiple donors attached to single acceptor and *vice versa*.¹³

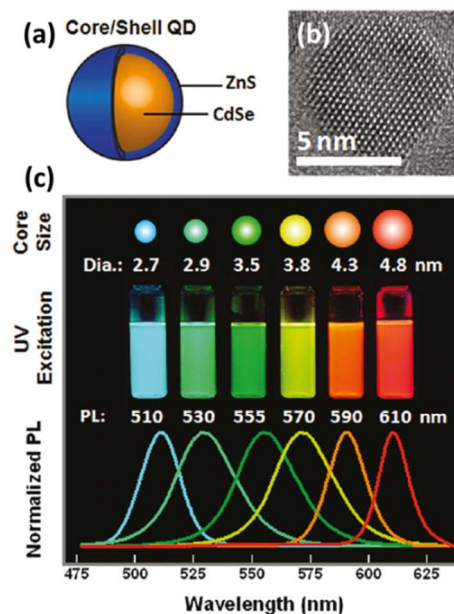


Figure 1 (a) Schematic drawing and (b) TEM image of CdSe-ZnS core-shell QD. (c) Illustrative size, photograph and photoluminescence spectrum showing progressive colour change of CdSe-ZnS QD with increasing

diameter. Reprinted with permission from ref. 13, © 2011 American Chemical Society.

For many as-synthesized QDs, surface modification is necessary to improve their biocompatibility. There are two general strategies for modifying QDs surface, namely ligand exchange and surface coverage.³⁸⁻⁴² In the former, bifunctional linker molecules are utilized to replace the hydrophobic capping agents on the as-synthesized QDs, affording both introduced aqueous stability and extra functional groups for further functionalization.⁴² In the latter, QDs hydrophobic surface is simply shielded by an additional layer of amphiphilic molecules, possibly also with a protective semiconducting shell in between.^{34,40} Some compositional elements of QDs, like Cd, are widely considered cytotoxic, hindering much of their practical applications, especially *in vivo*.⁴³ However, no consensus on QDs cytotoxicity has been concluded so far,⁴⁴ as there have been reports in which cytotoxicity is detected,⁴⁵ but also others in which it is absent.^{46,47} Bottrill and Green recently reviewed various aspects of QDs cytotoxicity, and concluded with an optimistic outlook about the future of QDs in biotechnology.⁴³ One effective way to tackle the cytotoxicity problem is perhaps to encapsulate QDs with nontoxic layers (e.g., silica and ZnS).⁴⁸ On the other hand, QDs made of cytotoxicity-free or less toxic materials, such as Si, InP and InGaP, could be another antidote to the cytotoxicity problem.⁴⁹⁻⁵²

Metal Nanoparticles

Metal nanoparticles (mNP), particularly gold nanoparticles (AuNP), have long been attractive transducing elements for biosensor design, by virtue of their facile synthesis, non-linear optical property, fluorescence quenching and enhancement capability, as well as the versatile surface chemistry.^{17-20,53} A detailed discussion on the AuNP synthesis, surface functionalization, physical and chemical properties can be found in ref. 20. In favour of colloidal stability, AuNP surface has to be covered with capping agents like the citrate ions (

Figure 2 a).⁵⁴ These agents can be further replaced by other desired substances like oligonucleotides, peptides, polymers and proteins, which establish the foundation of AuNP versatility for biological applications. Optical absorption of colloidal AuNP solution is governed by the well-known Localized Surface Plasmon Resonance (LSPR) (

Figure 2 b). Originated from LSPR, two types of colorimetric biosensors have been well developed, relying on particle aggregation and change of ambient dielectric constant principles, respectively. Under aggregation principle, it can be further divided into crosslinking⁵⁵⁻⁵⁸ and non-crosslinking⁵⁹⁻⁶⁴ schemes. Mirkin and co-workers⁵⁵ pioneered the crosslinking research and were able to detect femtomolar (fM=10⁻¹⁵ M) level oligonucleotide target in solution. Lu and co-workers further advanced this field with reversed colour change using DNAzyme or aptamer as the sensing probe, which is able to cleave the substrate when cofactors (e.g. Pb²⁺, Uranyl) are in presence, or able to interact with target to dehybridize the crosslinker that initially connects neighbouring AuNPs.⁶⁵⁻⁷⁰ Alternatively in the non-crosslinking scheme, analytical target possesses the capability of agitating the colloidal stability and allows van der Waals attraction to irreversibly aggregate AuNPs. In the second design principle that relies on the ambient dielectric constant change, adsorption of complexes

onto AuNP surface is able to red-shift the LSPR band.⁷¹ Such band shifting depends on the adsorbent layer thickness but produces very limited colour change. Therefore, microplate readers might be needed to show the differences in the light absorption spectra.

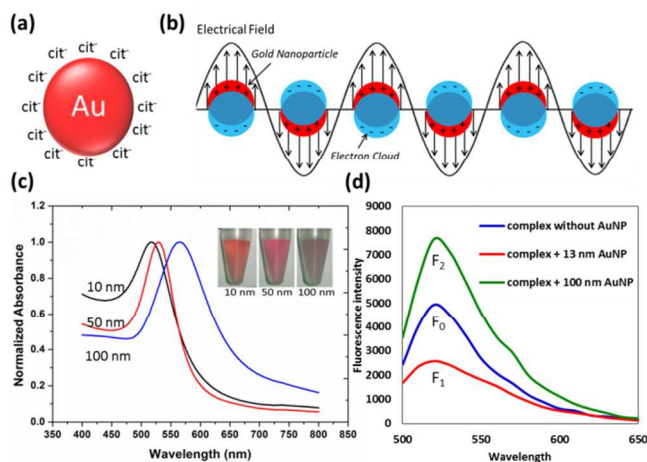


Figure 2 (a) Schematic drawing of citrate-capped AuNP; (b) Simplified illustration of localized surface plasmon resonance, where the free electrons in conduction band are driven into oscillation due to the coupling with electrical field of incident light; (c) Aqueous absorbance spectra of citrate-capped AuNPs with diameters of 10 nm, 50 nm and 100 nm (inset is the digital photograph of AuNP solution); (d) Effect of the fluorescence quenching (curve F1, for 13 nm AuNP) and enhancement (curve F2, for 100 nm AuNP) for FAM-contained complex. Panel (d) is reprinted with permission from ref. 71, © 2014 Springer.

It is worth highlighting that optical behaviour of mNPs actually has two components: absorption and scattering that are responsible for fluorescence quenching and enhancement, respectively (

Figure 2 d). Both of them are favourable for the biosensor construction with dual transducing elements, benefit from their capabilities of modulating proximal fluorophore emission. For example, AuNP of proper size is able to silence the neighbouring fluorophore over much longer distance than that for organic quenchers, rendering itself the great competence as superquencher in those fluorescence based dual-transducer designs. In addition, versatile surface chemistry of AuNP is another contributing factor for its prominent excellence. Thiol-containing molecules have demonstrated great suitability as anchor onto AuNP, by virtue of strong thiol-Au interaction and availability of thiol groups in many biomolecules and organic compounds. For instance, cysteine-tagged peptide are being widely utilized to functionalize AuNP for different applications, including aqueous stability enhancement, matrix metalloproteinase (MMP-7) detection, botulinum neurotoxin sensing, as well as the gene regulation.⁷²⁻⁷⁵

Upconversion Nanoparticles

Upconversion describes a phenomenon in which fluorophore is excited at longer wavelength and then give off shorter wavelength emission.⁷⁶⁻⁸⁰ Since most inorganic crystals do not demonstrate such property, attention is mainly focused on a

particular system that comprises crystalline host and lanthanide dopants (Figure 3 a and b).⁷⁷ Detailed discussion on the upconversion nanoparticles (UCNPs) synthesis, surface modification, fluorescence tuning and various applications in biological research can be found in ref 77 to 80. For a given host matrix like NaYF₄, by carefully changing lanthanide dopant combination and concentration, the emission can be finely tuned from visible to near infrared (NIR) region upon single wavelength excitation (Figure 3 c and d).^{81,82} However, it is also of note that host matrix does play an important role in the overall optical behaviour. For example, it has been found that the hexagonal phase (β) NaYF₄ exhibits order of magnitude higher quantum efficiency than the cubic phase (α).⁸³

Despite various synthetic approaches for diverse UCNPs morphologies,^{76-78,84-86} many of them only produce the hydrophobic surface that cannot be directly used for biological applications. Currently in literature, two strategies are available for UCNPs surface modification, namely encapsulation with SiO₂ or amphiphilic copolymers and replacement of original organic layer with hydrophilic ligands.⁸⁷⁻⁸⁹ Such concept is similar with QDs surface modification that has been discussed in that corresponding section.

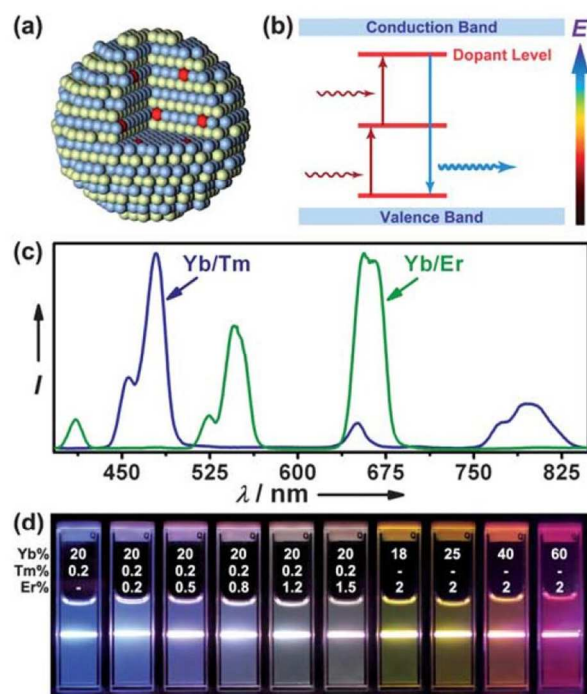


Figure 3 (a) Schematic drawing of UCNPs with lanthanide dopant ions embedded in nanocrystal host, (b) Simplified energy level diagram for the energy transfer mechanism between different lanthanide dopants, (c) Emission spectra of NaYF₄: Yb/Tm (20/0.2 mol%) and NaYF₄: Yb/Er (18/2 mol%), (d) UCNP emission colour tuning by varying the dopant combination and concentration. Panel (a) and (b) are reproduced with permission from ref. 90, © 2010 Royal Society of Chemistry. Panel (c) and (d) are reprinted with permission from ref. 82, © 2008 American Chemical Society.

As a new class of luminescent material, UCNPs have drawn much scientific attention, and widely considered as promising alternative to organic dyes and QDs for diverse applications. They offer tunable luminescence wavelength, high quantum

yield, as well as excellent photostability. Therefore, those well-established biosensor design principles for QDs and organic dyes can be extended to UCNPs with ease. More importantly, the anti-Stokes shift allows infrared (IR) or near infrared (NIR) excitation, which can significantly lower the interfering noises from background and also increase the penetration depth.⁹⁰ All these characteristics make UCNPs much suitable for bioanalytical studies in complex medium or even *in vivo*. Nevertheless, coupling UCNP with other transducing elements (e.g., luminescent reporters and fluorescence quenchers) facilitates more design versatility possibly with further enhanced sensing performances.

Graphene, Graphene Oxide and Carbon Nanotube

Graphitic material is not new provided its wide usage as pencils, lubricants and electrical conductors. However, after the Nobel Prize winning study on single- or bi-layer graphene,⁹¹ enormous attention has been re-focused on this star material as well as its various derivatives like graphene oxide (GO) and carbon nanotube (CNT). Thanks to their diverse favourable properties,⁹²⁻⁹⁴ graphene-derived nanomaterials have drawn enormous attention for biological studies including biosensors, disease diagnosis, drug delivery and cell imaging.^{95,96}

Despite the intact graphene that has been successfully synthesized via many approaches,^{91,97-103} it is the graphene oxide that attracts more attention in biosensor studies (

Figure 4 a). The epoxy, hydroxyl and carboxyl functional groups not only allow more versatile surface functionalization, but also contribute to excellent aqueous solubility and biocompatibility. Carbon nanotube, as inferred by the name, is in cylindrical configuration.^{104,105} Further classification divides CNT into single-walled carbon nanotube (SWNT) and multi-walled carbon nanotube (MWNT) based on their specific structures (

Figure 4 b).¹⁰⁶ It is of particular note that the functional groups on CNT mainly locate at the end tips, leaving the side walls highly aromatic.

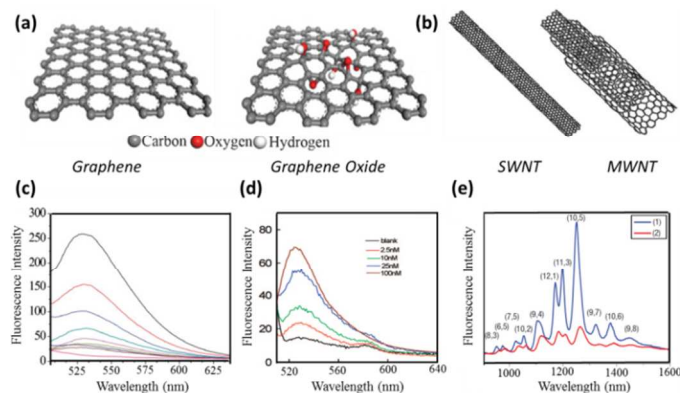


Figure 4 (a) Schematic structure of graphene and graphene oxide. (b) Schematic structure of single-walled carbon nanotube and multi-walled carbon nanotube. (c) Illustration of GO quenching: fluorescence spectra of 50 nM FAM in the absence (black curve) and presence of GO with various concentrations (from top to bottom: 5, 10, 15, 20, 25, 30, 35 µg/mL). (d) Illustration of CNT quenching: fluorescence spectra of 50 nM ssDNA-tethered FAM in presence of CNT quencher and various concentration of target DNA (target DNA can hybridize with ssDNA probe, and recovers the FAM fluorescence from CNT quenching). (e)

SWNT fluorescence spectra in absence (Curve 1) and presence (Curve 2) of quencher. Panel (a) is reproduced with permission from ref. 103, © 2008 WILEY. Panel (b) is reproduced with permission from ref. 107, © 2007 Elsevier. Panel (c) is reprinted with permission from ref. 108, © 2010 WILEY. Panel (d) is reprinted with permission from ref. 109, © 2008 American Chemical Society. Panel (e) is adapted with permission from ref. 110, © 2007 Nature Publishing Group.

In dual-transducer based biosensors, GO and CNT mainly perform as fluorescence quencher, working cooperatively with various fluorophores and sensing probes for both “light-on” and “light-off” sensor construction (

Figure 4 c and d). Among many of the demonstrated characteristics, different binding affinities towards ssDNA and dsDNA are of intensive consideration. By virtue of the accessibility of nucleobases in flexible ssDNA sequences, they can easily adsorb onto the aromatic surface; whereas the rather rigid phosphate backbone in dsDNA hinders its effective binding with aromatic basal plane. Stemming from such affinity difference, many novel biosensor designs with dual transducing elements have been reported. Of some specially cases, biomolecules in vertical orientation can also be established onto the aromatic surface, with assistance of linkers or specially designed functional groups.¹¹¹ Crosslinking-based sensing principle can therefore be employed.

Despite the similarities, GO and CNT also differ in many aspects. A thorough and detailed comparative study was reported by Braet and co-workers recently, with particular focus on material structures, properties and applications in biosensor design.¹⁰⁵ Although most GO or CNT-based optical assays are relying on fluorescence quenching phenomenon, there are also examples in which GO/CNT enzyme-mimicking catalytic capability and CNT NIR photoluminescence (

Figure 4 e) are employed for biosensor construction.^{105,110,112}

Carbon Nanodots

Carbon nanodots (CDs), as a new class of carbon allotrope material, have attracted much scientific attentions worldwide.¹¹³ Most CDs are quasispherical nanoparticles (<10 nm in size) with numerous carboxylic acid moieties on surface (Figure 5 a and b). They inherit the favourable characteristics of QDs including emission tunability and photobleaching resistance, but exempt from the shortcomings that conventional QDs suffer from. Following its serendipitous discovery in 2004,¹¹⁴ many synthetic approaches have been developed for effectively fabricating CDs of different sizes and surface functional groups.^{115,116}

The carbon atoms within CDs have great sp² character that indicates its nanocrystalline graphite signature. Typically, CDs demonstrate strong absorption in the UV region, with a tail well extended to the visible part.¹¹⁷⁻¹²¹ Although origin of CDs photoluminescence is not yet fully understood, accumulating evidences point to the fact that it arises from the radiative recombination of excitons located at surface energy traps.¹¹⁷⁻¹¹⁹ Similarly, mechanisms behind CDs surface passivation and quantum yield are also not clear at this moment and require more efforts to devote in.¹²¹⁻¹²⁴

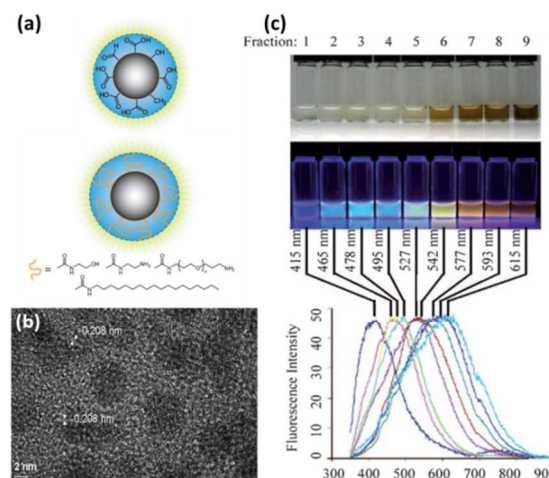


Figure 5 (a) Schematic drawing of carbon nanodot after surface oxidative treatment and further functionalization with surface-passivation agents. (b) High resolution TEM image of carbon nanodot. (c) Photograph of polyacrylamide gel electrophoresis (PAGE)-separated carbon nanodot produced from candle soot under white and UV excitation, as well as the corresponding fluorescence emission spectra. Panel (a) is reproduced with permission from ref. 115, © 2010 WILEY. Panel (b) is reprinted with permission from ref. 122, © 2009 American Chemical Society. Panel (c) is adapted with permission from ref. 124, © 2007 WILEY.

Recently, various studies on CDs have demonstrated many of their biologically favourable characteristics, such as photostability and tunable photoluminescence.¹²⁵⁻¹³³ As a promising alternative to QDs, CDs contain no cytotoxic element, rendering more application possibilities in biotechnology, especially in the cases involving live cells or *in vivo* studies. In addition to the well-established role as bioimaging labels, the dual-transducer biosensor design has witnessed CDs involvement as FRET donors and acceptors,¹³⁴ as well as enzyme mimics for chemiluminescence reactions.¹³⁵ The use of CDs in biosensor research just starts to emerge. By virtue of all the favourable characteristics discussed above, intensive explorations and many more appealing achievements can be expected in near future.

Mechanisms and Applications of Dual-Transducer Principles

As aforementioned, a typical biosensor features two fundamental components: *sensing probe* for target recognition, and *transducing element* for transforming biological binding events into detectable signals. The target recognition step is generally relying on the bioaffinity interactions, including but not limited to the reactions between complementary nucleic acid strands, antibody and antigen, aptamer and target, biotin and avidin, enzyme and substrate, as well as DNA molecules and their binders (e.g. drugs, metal ions, and proteins). These specific interactions are then transduced into the change of fluorescence intensity and/or polarization, solution colour, or some other optical signals. Such signals are readily detectable using ordinary lab equipment and even naked eyes in some cases. In this section, dual-transducer based biosensor designs are to be discussed. The content is organized according to the transducing mechanisms, namely Förster Resonance Energy Transfer (FRET), Amplified Fluorescence Polarization (AFP),

Bio-barcode Assays (BCA) and Chemiluminescence (CL) principles. With the assistance of schematic drawings of various assay principles and representative examples, we attempt to provide an overall picture of the dual-transducer based biosensor research, with particular focus on the general design rules and respective performances for the desired target analytes.

Förster Resonance Energy Transfer (FRET)

Förster Resonance Energy Transfer (FRET) was firstly reported by Theodor Förster in 1948.¹³⁶ It describes an energy transfer mechanism between proximal fluorophores via transition dipole-dipole coupling. Given aligned dipole orientation and proper overlap between donor emission and acceptor absorption, energy transfer efficiency follows the correlation of $1/[1+(R/R_0)^6]$. R is distance between donor and acceptor. R_0 is Förster radius defined as distance at which 50% energy is transferred. This radius is a function of ambient refractive index, degree of spectra overlap, quantum yield of donor-acceptor pair, as well as the dipole-orientation factor. Due to the inverse 6th power relationship, small variation of the inter-fluorophore distance can lead to a tremendous change in the energy transfer efficiency. This makes FRET a sensitive and convenient technique for sensing the distance variation and conformational change of biomolecules. However, the effective FRET distance is less than 10 nm, which is usually too short for large proteins, protein complexes or DNAs of moderate length.¹³⁷ Therefore, it is of great desire to increase the distance over which effective FRET can occur. Theoretical work done in the 1980s suggested noble metal particles are able to improve the FRET efficiency of its proximal donor-acceptor pairs.¹³⁸ Experimentally, Lakowicz and co-workers demonstrated that by attaching a silver nanoparticle (20 nm diameter) onto donor, Förster radius can be increased from 8.3 to 13.0 nm and FRET rate constant near the particle is found 21 times higher than that without the silver nanoparticle.^{139,140}

Though FRET was originally defined as the energy transfer phenomenon between two fluorophores,^{136,141} nowadays researchers tend to name a system FRET as long as the fluorescence energy is transferred to a proximal unit; no matter it is fluorophore or fluorescence quencher.¹⁴² To avoid any ambiguity in this review, we follow the latter definition of FRET, in which energy transfer could happen in either fluorophore/fluorophore or fluorophore/quencher combination. Of note, the FRET efficiency between fluorophore and metallic quencher is inversely related to the 4th power of the distance, instead of 6th in the conventional design.¹⁴³⁻¹⁴⁵ This is possibly due to the surface isotropic distribution of the dipole vectors on metal nanoparticle. Such energy transfer is sometimes referred as nanosurface energy transfer (NSET).¹⁴⁶ Herein, we merely treat it as a sub-category of FRET. To quantify the quenching effect, plots of donor fluorescence intensity change I/I_0 and quenching efficiency $(1-I/I_0)$ are commonly utilized, in which I_0 and I are the donor fluorescence intensities in absence and presence of the quencher, respectively. In some cases, the fluorescence data can also be fitted into the Stern-Volmer equation, $(I_0/I)-1=K_{SV}C_A$, where C_A is the quencher molar concentration and K_{SV} is the corresponding Stern-Volmer quenching constant.¹⁴⁷ However, it is worth mentioning that such Stern-Volmer relation is more commonly used to describe diffusion-driven collision between the donors and acceptors.

Given the flourishing research on nanomaterial,¹⁴⁸⁻¹⁵⁰ FRET, as a flexible fluorescence-based design principle, has been

customized into various configurations for much wider applications than ever before. This results in the exceedingly larger quantity of FRET related literature than the other three dual-transducer mechanisms in later sections. To make these versatile FRET designs easy to follow, discussions in this section is divided into three parts according to their sensing target, including metal ions and small molecules, DNA, proteins and enzymes. In each part, schematic drawings are provided to illustrate how the presence of analyte can be transduced into detectable signals. As a general trend, quenching-based principle is more preferentially applied, mainly because of its higher energy transfer efficiency than the conventional designs with energy transferred from one fluorophore to the other. In addition, light-on assay is usually more sensitive than the light-off, due to its smaller standard deviation (δ) of the blank sample signal. Such δ value is often used to calculate the limit of detection according to the 3δ rule.

Detection of Metal Ions and Small Molecules In view of the important roles of metal ions and small molecules in physiological activity, development of facile and sensitive biosensors for such target has been a topic of extensive study for decades. In principle, FRET system consists of donor and acceptor, as well as sensing probe(s) that associate them in a preferred manner. Unlike those analytes with special properties (e.g. multiple binding sites and complementary binding), metal ions and small molecules usually do not have much versatility in reacting with the sensing probes. Bioaffinity competition (Figure 6, scheme A and B) and sensing probe cleavage (Figure 6, scheme C and D) are therefore two of the most commonly utilized designs. Under each design, customized configurations are made available to accommodate the specific needs arising from target analyte characteristics, nanomaterial availability, sensitivity tolerance, and equipment restrictions.

Table 2 summarizes some of the representative examples of FRET biosensors for metal ions and small molecules detection, in terms of their design schemes and performance.

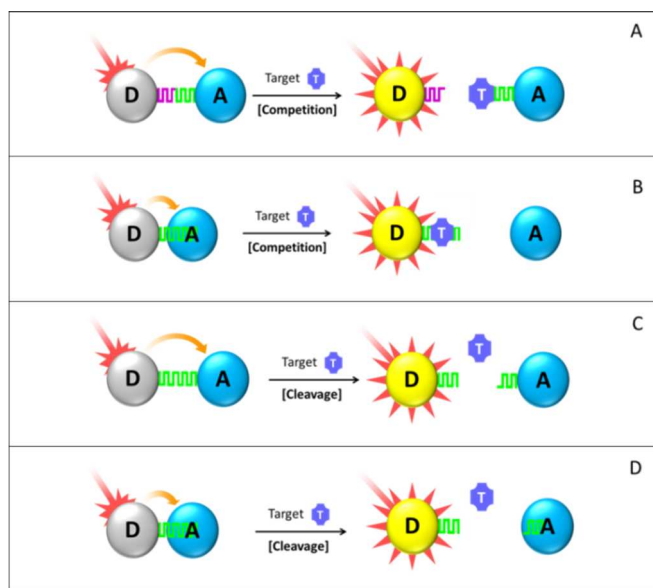


Figure 6 Schematic drawings of FRET biosensors for detecting metal ions and small molecules: (A & B) competition-based assays with crosslinking and nonspecific adsorption-based FRET configurations respectively; (C & D) cleavage-based assays with crosslinking and nonspecific adsorption-based FRET configurations, respectively. In principle, the positions of donor “D” and acceptor “A” are interchangeable in all cases. The drawings are not representing actual dimension of the respective biosensor components.

In bioaffinity competition assay, FRET system has to be carefully designed to fulfil the following two requirements. First, in absence of target analyte, energy transfer between donor and acceptor is well facilitated and donor fluorescence is readily quenched. Second, analyte/probe interaction has higher binding constant than donor/probe or acceptor/probe combination, so that added target analyte is able to displace donor or acceptor out of the FRET system and recover the donor fluorescence subsequently. Based on the interaction between sensing probe and donor/acceptor, such design principle can be further categorized into two cases. In the first (Figure 6 scheme A), donor and acceptor are functionalized with their respective sensing probe (e.g. Concanavalin A and thiolated β -cyclodextrins,¹⁵² cysteamine and 11-mercaptoundecanoic acid¹⁵⁴) or single molecule with two distinctive epitopes (e.g. 18-crown-6 ether,¹³⁴ β -cyclodextrin¹⁵¹) that are able to bring donor and acceptor into FRET-sensitive distance in the initial state. Then by displacing donor or acceptor out of the established FRET system, added target analyte helps to recover the quenched donor fluorescence. Of note, competition herein occurs between analyte target and the sensing probe, which does not destroy the pre-assembled donor-probe or acceptor-probe conjugate.

In the second case, association between sensing probe and acceptor (or donor) is achieved via nonspecific interaction (Figure 6 scheme B). Target analyte then competes with sensing probe to non-specifically bind with acceptor. Such design is mainly employed in the cases where the sensing probe is linear biomolecule like ssDNA, and the acceptor contains aromatic surfaces. Interaction between ssDNA and aromatic

surface is mainly via π - π stacking and hydrophobic reaction between nucleobases and the aromatic rings. The mechanically flexible structure of ssDNA makes its nucleobases readily accessible for the nonspecific stacking, whereas those in dsDNA are shielded by the rigid phosphate backbone, resulting in poor structure accessibility. Therefore, in presence of aromatic surface, ssDNA can be adsorbed but not for dsDNA (see

Figure 7). Provided such affinity difference, target detection can be achieved if it is able to induce DNA structural change from single-stranded to double-stranded or hairpin shape. Example of this design could be the Hg^{2+} and Ag^+ detection using ssDNA sensing probe.^{108,161,163} Hg^{2+} and Ag^+ can hybridize T-rich and C-rich mismatched ssDNA sequences, respectively. The presence of target ion can therefore be translated into reduced binding affinity due to the ssDNA-to-dsDNA transformation, and further to the recovered fluorescence intensity of the ssDNA-tagged fluorophore. Moreover, utilization of aptamer as sensing probe further emphasises the significance of such affinity change, making it capable of detecting various target analytes, including ATP, adenosine, small molecular drugs and peptides.^{108,165,166} Aptamer, with the name coming from Latin *aptus* (meaning “fit”) and *meros* (meaning “part”), has emerged in recent years as a powerful and versatile sensing probe material. It exhibits antibody-comparable selectivity but with more robust structure. Many of the commonly used aptamers are ssDNA and they behave just like ordinary oligonucleotide if target is in absence. While upon interacting with target analyte, it will undergo significant conformational change, wrapping around the target or forming hairpin structures. These restricted structures have much reduced aromatic binding affinity due to poor accessibility of the nucleobases, as discussed before. Of particular interest, in some other special cases sensing probe can be omitted and donor-acceptor association is realized solely via their surface ligand interaction. For example, direct mixing of unmodified AuNP with Rhodamine B (RB) leads to significant RB fluorescence quenching due to its binding with AuNP. Hg^{2+} target is able to displace the RB molecule out of the AuNP-RB composite and recover its fluorescence intensity in a Hg^{2+} concentration-related manner.¹⁵⁷

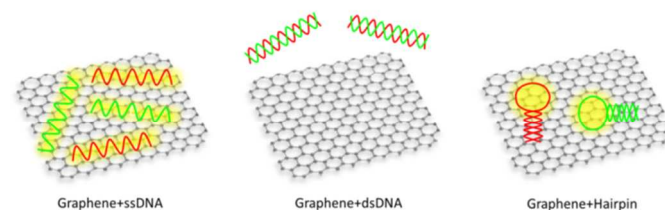


Figure 7 Interaction of graphene with ssDNA, dsDNA and hairpin structured DNA. ssDNA is able to adsorb onto the aromatic graphene surface (left); dsDNA shows little affinity (middle); hairpin structured DNA demonstrates moderate binding affinity due to the simultaneous presence of single-stranded and double-stranded portions.

In the probe cleavage-based assay design (Figure 6 scheme C and D), added target analyte possesses capability of digesting sensing probes that connect donor and acceptor in the pre-established FRET system.^{168,169} Following such digestion, the FRET system is largely disturbed and donor fluorescence is therefore recovered with increment value directly proportional to target concentration. Aforementioned classification based on the ways of probe-acceptor association still applies here. In

scheme C, the two epitopes of sensing probe are anchored onto the donor and acceptor surface. Hence, probe cleavage does not involve any on-particle reaction as cleavage site is on the sensing probe. Yet in scheme D, sensing probe is non-specifically adsorbed onto one of the FRET components (e.g. acceptor), which leads to the probe-cleavage happening on acceptor surface although cleavage site still locates on the sensing probe itself. As strength of nonspecific binding is proportional to the length of sensing probe (e.g. ssDNA or polypeptide), the shortened probe fragment after cleavage is no longer able to retain the donor into close proximity with acceptor.¹⁷¹ Therefore, it departs and has the donor fluorescence greatly recovered. However, one has to pay special attention that such probe cleavage assays are intrinsically limited to the target analyte which possesses probe-cleaving capability. To further broaden the application spectrum, enzymes or equivalent substances that are able to digest certain substrate can be introduced. The enzymes have to be well selected to make sure enzymatic digestion only occurs in presence of specific cofactors (e.g. metal ions, small molecules). With the help of such enzyme, presence of target analyte is surrogated by the donor fluorescence recovery although the donor-acceptor linkage is not directly cleaved by the target metal ions or small molecules. As an illustrating example, Zhang and colleagues reported a Pb²⁺ detection assay with 300 pM LOD, using FAM donor, GO quencher and DNAzyme substrate as sensing probe.¹⁷¹ The used GR-5 DNAzyme is not activated until Pb²⁺ is added in, which then assists the substrate cleavage and FAM fluorescence recovery.

Bearing in mind the above-discussed principles, some useful guidelines can be drawn to guide the design of FRET biosensors for metal ion and small molecule in general. First, most of the reported LOD falls in the range of micromolar ($\mu\text{M}=10^{-6}$ M) to nanomolar ($\text{nM}=10^{-9}$ M), with some down to picomolar ($\text{pM}=10^{-12}$ M). Beyond this range, FRET might not be a suitable method and some other options have to be considered. This limitation may arise from the intrinsic nature of FRET, either light-on or light-off without further signal amplification. Second, although no overall advantages can be claimed for any of the four design principles shown in Figure 6, some points are still worth highlighting. For example, with adenosine as modal target, scheme B possesses much lower LOD than scheme A (10 μM vs. 50 μM),^{108,155} mainly because aptamer-GO interaction is much weaker than aptamer-ssDNA hybridization, which makes it easier for target adenosine to interact with aptamer in the scheme A design. On the contrary, lower sensitivity of scheme A than scheme B (10 pM vs. 0.5 nM) is observed when looking at Hg²⁺ as target analyte.^{157,163} This might be due to the fact that, the oligonucleotide-modified UCNP in scheme B are adsorbed onto GO by multitude contacting points, so that multiple Hg²⁺ are required to free one UCNP from the GO quenching. However, in scheme A the Hg²⁺-RB displacement may follow a lower ratio. Third, GO and AuNP are commonly used as FRET acceptors by virtue of their high quenching efficiency and well understood chemical and physical properties. As for the donors, nanometer-sized fluorophores (e.g. UCNPs,¹⁶³ QDs^{152,155} and CDs^{134,158}) start to play active roles despite the still dominant usage of organic dyes (e.g., FAM,^{108,161,162,165,168-171} cyanine dyes,^{68,164} Rhodamine B^{156,157}). Fourth, given similar conditions, biosensors with nanomaterial donor (e.g., UCNPs) demonstrate superior sensitivity over those with organic dyes.^{108,163,165} UCNP has much lower fluorescence background because of its IR or NIR excitation. Therefore, detection sensitivity can be

significantly improved because the LOD is often calculated using 3δ rule where δ is the standard deviation of background signal. Fifth, use of aptamer as sensing probe is always worth thorough consideration for detecting metal ions and small molecules, especially for target analyte that does not possess any usable physical or biochemical properties. Structure-wise, many of the aptamers are merely ssDNA which can effectively interact with GO or CNT in a sequence-independent manner. Function-wise, it is able to specifically bind with desired target and undergo dramatic structural transformation. Such functional and structural characteristics make aptamer much suitable and attractive for the design of bioaffinity competition based FRET assays. Sixth, FRET system utilizing nonspecific association between sensing probe and acceptor (Figure 6 scheme B and D) oversteps their counterpart assays (scheme A and C) in terms of facile material synthesis and lower assaying cost, since only single labelling is required for probe modification. However, such merit can be balanced against the poor detection selectivity, particularly when target or sensing probe analogues are in presence, which is able to non-specifically disassociate the sensing probe out of the FRET system.

Relative to single-target detection, multiplexed assay also draws enormous attention due to its advantages of reduced analyzing time/cost and less amount of required sample volume. More importantly, it facilitates feasible, reproducible and reliable comparative analysis. As proof of concept, Fan, Song and co-workers proposed an aptamer-AuNP based multicolour design with adenosine, potassium ion and cocaine as modal targets.¹⁷² AuNP surface was functionalized with three types of DNA sequence that were complementary to the three utilized aptamers. Each type of aptamer was labelled by specific dye molecule. Initially, DNA hybridization between aptamer and AuNP-tethered oligonucleotide brought the dye molecules into close proximity with AuNP and therefore had the dye fluorescence readily quenched. However, in presence of target analyte, DNA dehybridization took place due to the higher binding affinity between aptamer and its corresponding target analyte. The respective dye fluorescence was therefore recovered in a target concentration-correlated manner. In view of the fact that disease diagnosis and biomedical study sometimes require the information from multiple targets for pattern recognition, multiplexed assays are thus becoming increasingly crucial to complement advances in healthcare application to monitor several physiological parameters or to detect various target analytes in one go.

Detection of DNA Molecules In general, FRET-based DNA biosensors can be categorized into six configurations (as shown in

Figure 8) that follow three basic design principles, namely target induced crosslinking (scheme A), DNA strand competition (scheme B, C and D) and DNA conformational alternation (scheme E and F).

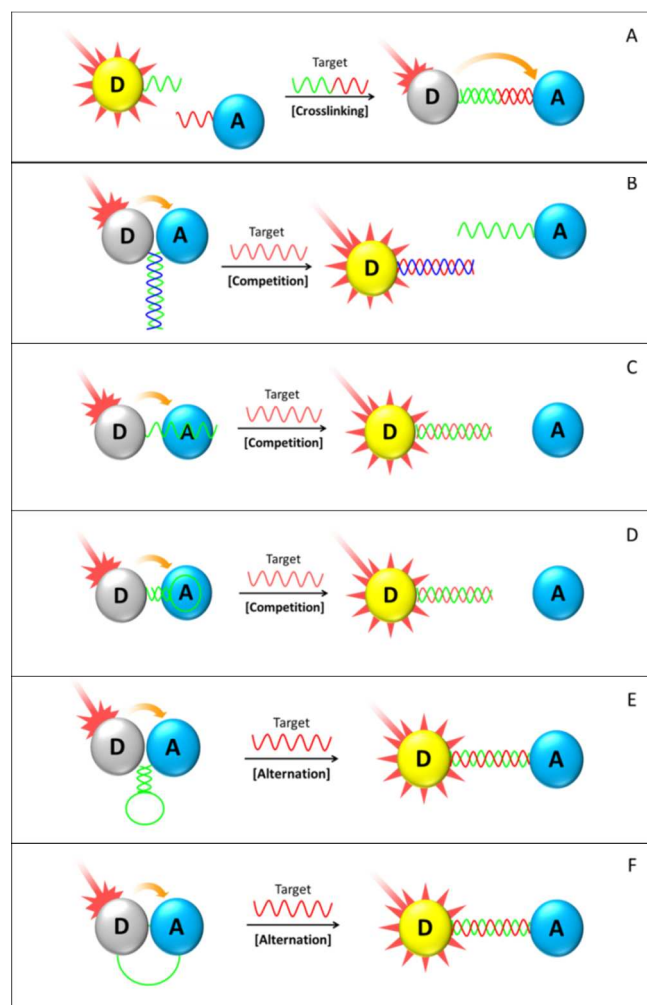


Figure 8 Schematic drawings of FRET biosensor for detecting DNA molecules: (A) DNA crosslinking light-off assay; (B-F) analyte induced light-on assays. (B, C & D) strands competition based assays with different acceptor attachment configurations; (E & F) DNA probe conformational alternation-based designs with hairpin and ordinary ssDNA sensing probes, respectively. In principle, the positions of donor “D” and acceptor “A” are interchangeable for all drawings. The drawings are not representing actual dimensions of the biosensor components

Target crosslinking mechanism generally leads to the light-off FRET assay, in which target addition results in the donor fluorescence quenching. In typical crosslinking design (scheme A), FRET donor and acceptor are modified with ssDNA sensing probes that have nucleobase sequences complementary with the target. Initially, appropriate excitation can only trigger signatory emission of the donor, because it is well separated from acceptor. Following the addition of target DNA, hybridization between sensing probes and target analyte takes place, crosslinking the donor and acceptor to form the sandwich-like structure. Such crosslinking brings donor and acceptor into FRET-sensitive distance, so that donor is able to transfer its fluorescence energy to the proximal acceptor and has its own fluorescence intensity significantly reduced.

Figure 8 scheme A is a drawing of the crosslinking principle using single donor-acceptor pair model. In practice, the system could have huge network structures due to multiple DNA

probes on the donor and acceptor surface. LOD of picomolar ($\text{pM}=10^{-12}$ M) to femtomolar level ($\text{fM}=10^{-15}$ M) has been reported by using either fluorophore/fluorophore or fluorophore/quencher crosslinking designs.^{111,173} It is also worth mentioning that such crosslinking could be easily applied for multiplexed target detection using different sensing probes and respective fluorophore.¹¹¹ Due to the high specificity of DNA hybridization, presence of certain target oligonucleotide can only lead to the fluorescence quenching of its corresponding donor while leave the others unaffected. Hence, it intrinsically imposes no negative influences on the detection limit for each individual target. Experimental results from Cui and co-workers have validated this point.¹¹¹

DNA strand competition assays (see scheme B, C and D) rely on the principle that added DNA target competes with transducing elements or sensing probes for binding with the others. In the first configuration (scheme B), both donor and acceptor are modified with ssDNA probe and the two probes are complementary with each other. Before target DNA addition, donor and acceptor are in close proximity via probe hybridization. Following the addition of target analyte that has identical nucleobase sequence with one of the probes, bioaffinity competition takes place and the pre-established FRET system is disturbed.¹⁷⁵ To further improve detection sensitivity, mismatched base pairs could be introduced into the hybridized probes. As perfectly complementary ssDNA target has a higher binding constant, it is able to displace more of the donors or acceptors out of the FRET system. The second configuration (scheme C) is based on the binding affinity difference between ssDNA and dsDNA towards aromatic acceptors (e.g. GO and CNT). ssDNA can be readily adsorbed onto the aromatic surface and has its tethered donor quenched. Following the target addition, dsDNA is formed and departs from the aromatic surface, and the donor fluorescence subsequently recovers. In addition, multiplexed target detection using competition principle has also been reported by Fan and co-workers using dye-labelled ssDNA as sensing probe and GO as common quencher by virtue of its large surface area for multitudes probe adsorption.¹⁰⁸ The third configuration (scheme D) is much similar with the second, except for the utilized hairpin sensing probe. As a special member of the DNA family, hairpin DNA structure has been intensively investigated regarding their working mechanism and diverse applications.^{184,185} Structure-wise, the hairpin DNA is oligonucleotide loop flanked by two self-complementary ssDNA tails. In the stem-close state, the self-complementary tails hybridize with each other, forming a “stem-loop” configuration. Target analyte then hybridizes with the loop portion, forcing the stem part to open up and inducing the formation of linear dsDNA. From stem-loop to dsDNA, its binding affinity towards aromatic surface decreases. Exploiting such decrease, DNA biosensors with LOD in the nanomolar ($\text{nM}=10^{-9}$ M) to picomolar ($\text{pM}=10^{-12}$ M) range have been constructed by several groups.^{108,109,176} However, one should be aware that stem part in hairpin structure becomes single-stranded after the target-loop hybridization. Therefore, ratio of nucleobase numbers in stem and loop portions have to be carefully designed to ensure the overall dsDNA percentage increase after hybridization.¹⁷⁷ In some particular cases, the ssDNA target also contains stem-complementary sequences, which leaves no dangling ssDNA tails after hybridization. Such design is kinetically favourable due to the elimination of ssDNA tails, but its practical application is much restricted

1 simply because the desired target oligonucleotide does not
2 necessarily contain the stem-complementary sequences.

3 DNA conformational alternation based design (see scheme E
4 and F) generally involves on-particle interaction without any
5 sensing probe cleavage or strand displacement processes. In
6 scheme E, hairpin DNA is dually labelled with donor and
7 acceptor at two far ends of the self-complementary tails. Hence,
8 donor fluorescence is quenched in the stem-close state because
9 of its proximity with acceptor. Such configuration is usually
10 termed as molecule beacon (MB) in literature.¹⁸⁴ Following the
11 addition of target DNA, sequence hybridization opens up the
12 stem-loop structure and pushes the donor far away from
13 acceptor. With donor fluorescence recovery, presence of target
14 analyte is therefore translated into the detectable optical signals.
15 Compared with assays using ordinary ssDNA probe, one of the
16 most significant advantages that MB-based design possesses is
17 probably the higher detection sensitivity towards base-pair
18 mismatch. However, several shortcomings are also identified,
19 including low quenching efficiency of organic quenchers,
20 complicated synthetic process and vulnerability to endogenous
21 nuclease degradation or corresponding DNA binder.^{186,187} To
22 address these challenges, especially the first two, various
23 nanomaterials have been thoroughly examined for their
24 potential roles in MB assay design. In 2001, it was the
25 Dubertret group that firstly used AuNP (1.4 nm diameter) to
26 replace the conventional organic quencher and successfully
27 constructed a novel MB-based sensor for ssDNA detection.¹⁸¹
28 Benefit from high quenching efficiency of AuNP, eight times
29 higher detection sensitivity towards single-base mismatch was
30 achieved. Fan and co-workers further improved such design by
31 using larger AuNP (15 nm diameter).¹⁸² More importantly, they
32 demonstrated the feasibility of detecting multiplexed target in a
33 single assay. In their hairpin-AuNP design, it is critical to
34 introduce the short “helper” oligonucleotides in between the
35 hairpin sensing probes on AuNP surface because of poor
36 aqueous stability of the hairpin-AuNP composite. Alternatively,
37 such nanometre-sized quenchers can also work cooperatively
38 with conventional MB, involving both the original organic
39 donor and acceptor.^{179,188} In addition to the improved LOD,
40 such nanomaterial-MB hybrid DNA sensor exhibits higher
41 thermal stability than the conventional MB counterpart, making
42 itself much suitable for biodetection tasks under stringent
43 experimental conditions.¹⁷⁹

44 Scheme F illustrates another DNA conformational alternation
45 based sensor design, utilizing ordinary ssDNA as sensing
46 probe. Some organic dyes (e.g. fluorescein) are able to
47 reversibly adsorb onto AuNP surface via ligand coordination or
48 electrostatic interaction.¹⁸⁹ Therefore, the ssDNA probe
49 connecting them is constrained into arch shape at initial state.
50 Upon target DNA addition, probe-target hybridization forms
51 the much more rigid dsDNA and dye molecule is separated far
52 away from AuNP surface. Donor fluorescence is therefore
53 recovered in a target concentration-dependent manner with
54 LOD around 40 nM at favourable conditions.¹⁸³ Compared with
55 hairpin-based assay shown in scheme E, this design possesses
56 advantages of facile material synthesis and low assaying cost,
57 whereas might suffer from sacrificed sensitivity for detecting
58 single base-pair mismatch, as well as the false positive signals
59 that arise from possible nonspecific interactions between
60 ssDNA probe and its various binders.

With target DNA of comparable length, it can be seen from

Table 3 that the crosslinking principle demonstrates higher sensitivity than the competition or probe alternation based designs, possibly because of the better accessibility of the sensing probe. In crosslinking (scheme A), the sensing probes on donor and acceptor surface are all extending outwards, making it much easier for target DNA to approach and bind with. Yet in the other designs, sensing probes initially all bind with some elements, involved in nonspecific interaction, complementary hybridization or structural restriction. This largely retards the efficiency of the desired target/probe interaction. Despite the advantageous detection sensitivity, crosslinking design suffers from tedious material synthesis (e.g., dual labelling) and high assaying cost. The same drawbacks also apply for the structure alternation-based assays (scheme E and F). As for the strand competition design (scheme C and D), only single labelling on the sensing probe is necessary, with the other labelling surrogated by nonspecific adsorption. However, DNA hybridization in the presence of GO or CNT takes much longer time than that in typical hybridization buffer. Elongated assaying time is detrimental to convenience of application and deteriorates the dye photobleaching problem as well. As discussed before, such nonspecific adsorption is also vulnerable to complex biological matrix and sensing probe analogues, which may lead to false positive signals. To add on, experiment stoichiometry involving DNA adsorption on aromatic surface has to be carefully selected, as there is evidence showing the remaining of dsDNA on SWNT surface after hybridization.¹⁹⁰

Detection of Proteins and Enzymes In this section, FRET biosensors for detecting proteins and enzymes will be discussed. Covered principles include bioaffinity competition, target induced crosslinking and enzymatic cleavage (see

Figure 9). Utilized sensing probes span from the small molecular ligands, aptamers, to (poly)peptides, and further to the protein-binding DNA molecules. The discussed enzymes in this review are mainly for peptide or DNA cleaving.

Bioaffinity competition assay for protein detection (

Figure 9 scheme A) is similar with that for detecting small molecules and DNA sequences described in previous sections. Both FRET donor and acceptor are functionalized with sensing probe that can specifically bind with each other, bringing them into FRET sensitive distance. Target protein is able to compete with one probe for binding with the other, which breaks the pre-established FRET system and recovers the donor fluorescence accordingly. As a representative example, biotin-avidin interaction has been well understood and commonly used for designing competition-based FRET biosensors.^{191,205} The reverse mechanism has also been employed, in which target analyte is able to crosslink donor and acceptor, hence establish the FRET system.²⁰⁶ Another design under competition principle (see scheme B1) involves usage of aptamer as sensing probe. The aptamer is anchored onto the donor surface at one end, but associated with the acceptor via nonspecific adsorption. Upon binding with protein target, aptamer undergoes dramatic structural change and loss its affinity towards the aromatic quencher. Donor fluorescence can therefore be recovered.^{176,192} Similar principle can be further adopted by using polypeptide sensing probe. However, the polypeptide has to be specially designed, so that it is able to interact with target protein and induce the formation of polypeptide-protein complex. Analogues with aptamer, such polypeptides also contain aromatic groups and demonstrate

high binding affinity towards aromatic quencher via π - π stacking. Formation of the polypeptide-protein complex much reduces the affinity and induces the donor fluorescence recovery.^{193,194} Moreover, hairpin peptide beacon (HPB), as sensing probe, has been proposed as well for protein target detection.²⁰⁷⁻²⁰⁹ HPB, similar with DNA molecular beacon (MB), comprises a protein-specific polypeptide loop flanked by two self-complementary peptide nucleic acid (PNA) sequences, as well as donor and acceptor tagged at the PNA far ends.²¹⁰ In absence of target protein, PNA hybridization brought donor and acceptor into close proximity and facilitate the donor fluorescence quenching. Protein target interacts with the central polypeptide sequence, opening up the hybridized PNA and forcing donor and acceptor far apart. As result, donor fluorescence intensity recovers. Superiority of HBP over MB is perhaps the possibility of removing the self-complementary PNA portion, leaving polypeptide conformational change solely dependent on the amino acid sequence and its interaction with target protein.²⁰⁷⁻²⁰⁹ Unfortunately, nanomaterial involvement in the HBP-based biosensor design is still lacking so far, and awaits intensive efforts to be devoted.

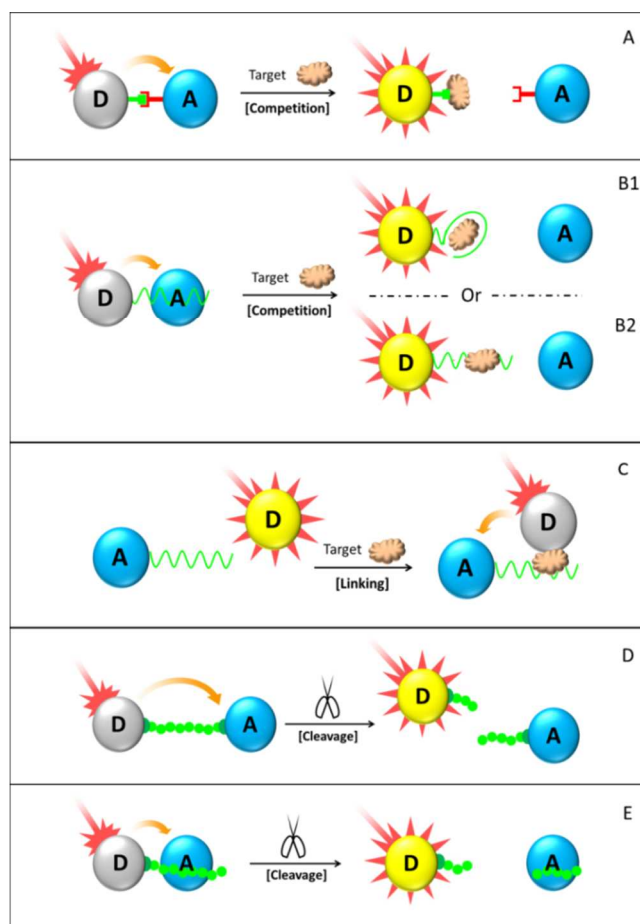


Figure 9 Schematic drawings of FRET biosensor for detecting protein molecules: (A & B) bioaffinity competition based light-on assays with crosslinking and nonspecific adsorption FRET configurations, respectively; (C) target-induced crosslinking light-off assay; (D & E) cleavage enzyme light-on assay with crosslinking and nonspecific adsorption configuration, respectively. The positions of donors and acceptor are interchangeable in all cases. The drawings are not representing actual size of the biosensor components.

Our group has recently developed a suit of hybrid sensors for detecting the protein-DNA interaction, using double stranded DNA-gold nanoparticle (dsDNA-AuNP) composite as acceptor and water soluble conjugated polyelectrolytes (CPEs) as donor.^{195,196} Both “light-on” (scheme B2) and “light-off” (scheme C) schemes are designed, in which CPEs fluorescence is recovered and quenched respectively upon adding in the corresponding target protein. Water soluble CPEs, as a new type of fluorescent material, have better competitive edge than the others by virtue of their high quantum yield, excellent light harvesting capability and more importantly, unique linear conformation. The involved CPEs have to be properly selected, so that their charge properties match well with dsDNA-AuNP composite and their emission wavelength overlap with the AuNP LSPR absorption. In principle, the protein target should bind with the dsDNA at specific DNA binding site, inducing change of electrostatic property of the dsDNA-AuNP composite. Such change modulates the composite electrostatic interaction with CPEs, leading to either stronger or weaker CPEs fluorescence quenching by AuNP. A “two-way” model, either “light-on” or “light-off”, is constructed as well, which allows the detection of protein with unknown charge properties. Experimentally, such principles have been exploited to study binding behaviour of various proteins (e.g. ER α , ER β , FoxA1, AP-2 γ) with their corresponding DNA binding site.^{195,196} It is further able to differentiate binding affinities of the two Estrogen Receptor (ER) subtypes (ER α and ER β), which have about 96% similarity in their DNA binding domain but substantially differ in physiological distribution and bio-functionality.¹⁹⁵ We also demonstrated that such hybrid sensors are highly sensitive to detect site- and nucleotide-specific single base variations on the ER α binding region. Screening of 15 singly mutations on the ER α binding site (3 possible substitutions in each of the 5 nucleobases of the binding site) gives rise to an *in vitro* binding energy model. Such model correlates well with the energy matrix obtained from *in vivo* genome-wide ER α binding data using Thermodynamic Modeling of CHIP-seq. This renders our assay design a highly reliable alternative for understanding *in vivo* protein binding mechanisms.

Enzymes, as a special group of protein molecules, are capable of catalysing biological reactions and/or induce structural change of their respective substrates. The malfunction of certain enzyme is usually responsible for severe biological abnormalities and disorders, which makes the design of enzyme sensors exceedingly important and highly desirable for diverse purposes. In the following discussion of this section, we will be focusing on the FRET assay designs primarily for peptide and DNA cleavage enzymes. According to the cleavage site, two commonly used sensor design configurations are elaborated, as shown in scheme D and E of

Figure 9.

In scheme D, donor and acceptor are linked via the linear sensing probe, whose length falls in the range of effective FRET distance. Donor fluorescence is therefore quenched at initial state. Target enzyme then digests the sensing probe at specific location, leaving two short fragments tethered on the donor and acceptor surfaces. Consequentially, the FRET mechanism collapses and donor fluorescence recovers. With appropriate cleavage substrate, detection of various enzymes including matrix metalloproteinase (MMP),^{197,198} caspase-3,¹⁹⁹ S1 nucleases,¹⁴⁶ as well as the multiplexed detection of various

targets in a single assay,²¹¹ has been well demonstrated with remarkable sensitivity, selectivity as well as rapidity. Alternatively, in scheme E sensing probe is associated with acceptor via nonspecific interaction. Due to decreased binding affinity, the shortened probe fragment is released back into the solution and has its tethered donor fluorescence recovered. LOD of 50 pM for MMP-2 was reported by Ma and co-workers using FITC donor, GO quencher and polypeptide sensing probe.²⁰⁴ This example confers such optical sensing design the sensitivity competitiveness over electrochemical, liquid chromatography and mass spectrometry approaches.^{212,213} Due to limited space, it is impractical to cover all assay designs here, even merely for peptide and DNA cleavage enzymes. However, the two design principles discussed above are widely used and lay the foundation of designing many other FRET enzyme biosensors.^{24,214-218}

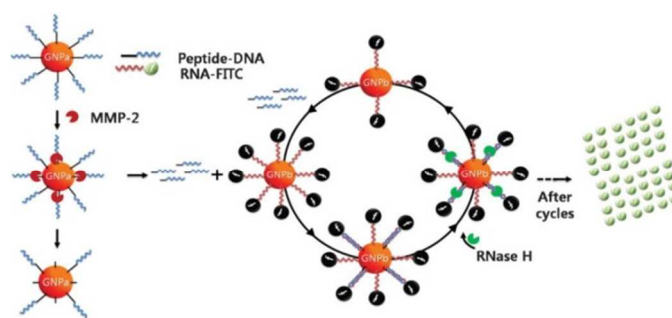


Figure 10 Schematic diagram showing the cascade procedure for fluorescence signal amplification. Reprinted with permission from ref. 219, © 2010 WILEY.

However, detection sensitivity and assaying rapidity of the above examples can never exceed the reaction kinetics between target enzymes and their substrates due to lacking of signal amplification. To resolve such limitation, Chung and co-workers proposed a cascade method involving DNA-peptide and DNA-RNA cleavages by MMP-2 and RNase H, respectively.²¹⁹ As shown in Figure 10, digestion of DNA-peptide composite by MMP-2 generates free DNA fragments. They are released from AuNP surface and enter the cycling loop to form heteroduplex with RNA molecules labelled by FITC. RNase H has no influence on single-stranded RNA but is able to degrade the RNA chain in the DNA/RNA duplex. Therefore, the FITC dye is disassociated from AuNP in the cycle and has its fluorescence intensity significantly recovered. Relying on such novel cycling loop for signal amplification, this design permits assessment of the MMP-2 activity at concentration of 10 pM within 4 hours, about 100-fold more sensitive and 2-time faster than the design without amplification. Such improvement results from the fact that RNase has higher turn-over rate and reaction affinity towards its substrate compared with MMP-2.

Amplified Fluorescence Polarization (AFP)

Fluorescence polarization (FP) or fluorescence anisotropy is a phenomenon in which fluorophore emission has unequal intensities along different directions. These two terms describe the same physical process, using different quantitative measurements with correlation shown below, where P denotes

the value of fluorescence polarization and r is the fluorescence anisotropy.²²⁰

$$r = \frac{2}{3} \left(\frac{1}{P} - \frac{1}{3} \right)^{-1}$$

Under light irradiation, fluorophore absorbs photons and excites itself to higher energy level. The absorbed energy is lost via photon emission and heat dissipation mechanisms after certain time period called “fluorophore lifetime”. Since excitation process involves redistribution of electrons about the fluorophore molecule, polarized excitation can only excite fluorophores along certain orientation. Subsequently, light is emitted in the same polarized plane, provided the fluorophores are kept stationary throughout excitation/emission process. However, fluorophores in aqueous solution undergo constant Brownian motion. They keep moving and rotating due to the thermodynamic collisions. In such case, light is emitted along different planes from polarized excitation and the difference is dependent on the relationship between fluorophore lifetime and rotational correlation time. The rotational correlation time of a fluorophore alone or a small complex is usually much shorter than the fluorophore lifetime. Hence, the fluorophores become randomly oriented and give off depolarized fluorescence emission. In contrast, polarized emission can be observed for fluorophore-containing complexes of a larger size, because of the longer rotational correlation time than the fluorophore lifetime. With an amplifier, the fluorophore-containing complex becomes even larger and the rotation is further slowed down, giving rise to more significant FP value (see Figure 11). Via such principle, size of the fluorophore-containing complex in micro-level is reflected by the FP value in macro-level. This makes FP principle highly suitable for biosensor design, because of the molecular binding and/or complex size change in many biological processes.^{221,222}

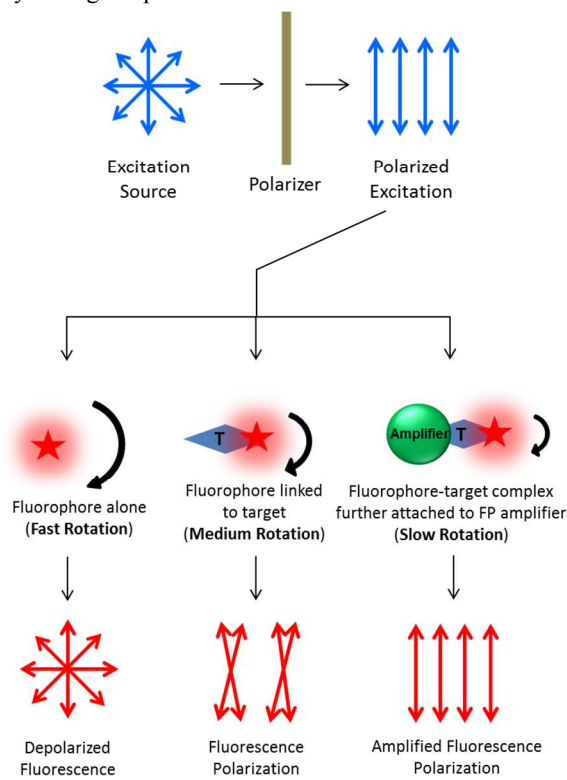


Figure 11 Schematic illustration of the fluorescence polarization principle and FP amplification mechanism. The curly arrow size indicates rotational speed of the corresponding complex.

For instance, dye-labelled aptamers have been readily utilized for quantitative analysis of biomolecules.²²³⁻²²⁵ Binding of target macromolecule with dye-labelled aptamer leads to much slower complex rotation and higher FP value. However, it is generally not applicable for detecting small molecules due to the limited size increase after target-probe binding. FP signal amplification is therefore required to make such design suitable for various targets detection, especially those of small size. One effective approach is to magnify the size difference before and after target binding. Thrombin, ssDNA binding protein and antibody have been widely reported in literature.²²⁶⁻²²⁸ In recent years, nanomaterial also starts to reveal their excellence for FP signal amplification. Such excellence stems from their tunable size/shape and superb interaction affinity with various biomolecules.

Six distinctive design principles of nanomaterial-amplified FP (AFP) assays are shown in

Figure 12 scheme A-F. In scheme A, target analyte has the capability to assemble sensing probes. These sensing probes are initially tethered onto the fluorophore and nano-amplifier, respectively. Without target analyte, FP value of the probe-tethered fluorophore is small. Following the target addition, formed complex contains both fluorophore and sensing probe, as well as the nano-amplifier. The overall size increases significantly and molecule rotational speed decreases, resulting in higher FP value relative to initial state. As an example, Hg^{2+} detection has been demonstrated using AuNP amplifier. By virtue of the capability of hybridizing T-rich mismatched ssDNA, Hg^{2+} helps to crosslink the FAM and AuNP amplifier, inducing a large increase in FAM FP value. LOD of 1.0 nM (0.2 ppb) was reported. As control group, LOD value was merely in micromolar (μM) range in the design without AuNP amplifier.²²⁹

In scheme B, initially the fluorophore is associated with nano-amplifier and the system displays high FP value. Upon adding in target analyte with probe digestion capability (e.g., enzymes or oxygen radicals), fluorophore and nano-amplifier are separated and overall FP value decreases subsequently.²³⁰ Moreover, other analytes such as enzymatic cofactors, can also be detected with the assistance of corresponding enzymes. Very recently, Huang and co-workers designed a FP-based Cu^{2+} detection assay using GO as amplifier and DNase as sensing probe.²³¹ The DNase cleaves substrate DNA only in presence of Cu^{2+} in nanomolar level. Other carbon-based nanomaterials (e.g. carbon nanoparticles and MWNT) were also tested as nano-amplifier. Yet their performance was inferior, possibly due to their low efficiency of releasing the cleaved DNA fragments.

In scheme C and D, aptamers are exploited as sensing probe for detecting small molecules. In the following discussion, we will use adenosine triphosphate (ATP) as model target to elaborate the detailed design principles.²³² As previously discussed, aptamer exhibits strong binding affinity towards aromatic surfaces, but such affinity largely decreases after aptamer-target interaction. Based on this principle, both “signal-on” and “signal-off” AFP-based designs are made available. The “signal-off” design (decreasing of FP value) is relatively simpler as it only involves GO amplifier and

fluorophore-tethered aptamer (see scheme C). Initially, aptamer sequence is adsorbed onto GO and the overall FP value is high. Upon target addition, formed aptamer-target complex departs from GO, leading to reduced FP value. As for “signal-on” design, additional ssDNA with dye labelling needs to be introduced (see scheme D). This ssDNA sequence is complementary with aptamer. Therefore, target-free condition gives rise to low FP value due to the low affinity of hybridized aptamer-ssDNA duplex towards GO. Following target addition, stronger aptamer-target interaction dehybridizes the duplex. Free ssDNA molecules then get adsorbed onto the aromatic surface and the overall FP value increases. Benefit from the highly selective aptamer, such AFP-based biosensors demonstrate excellent detection selectivity, even in presence of ATP analogues like UTP, CTP and GTP with much higher concentrations.²³²

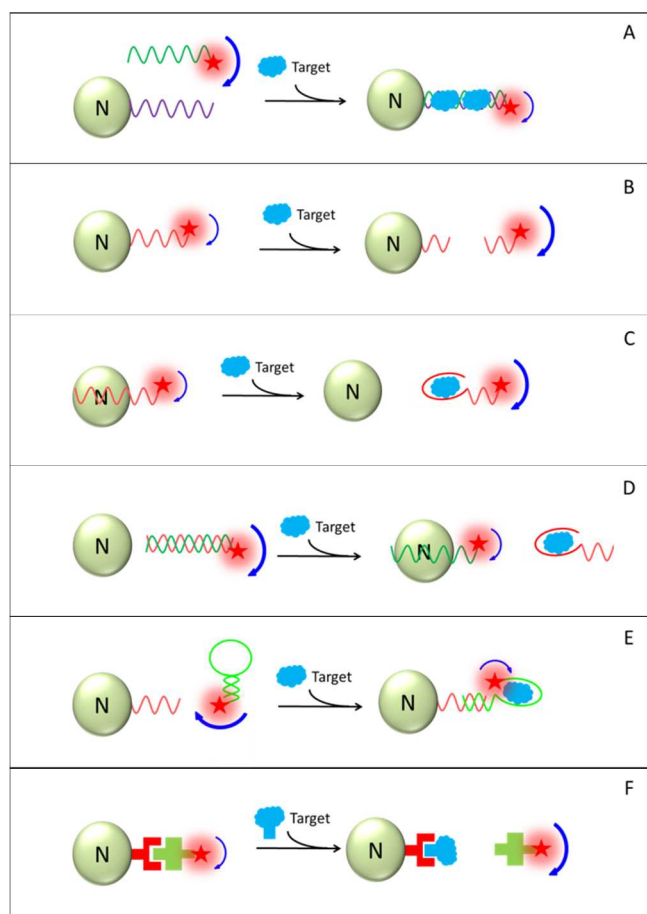


Figure 12 Schematic drawing of nanomaterial-amplified FP (AFP) assays, using principles of: (A) target-induced hybridization; (B) target-induced cleavage; (C) aptamer-based bioaffinity competition; (D) target-induced dehybridization; (E) hairpin-based bioaffinity competition; (F) target-based displacement. “N” stands for the utilized nanomaterial. The drawings do not reflect actual dimension of the biosensor components.

Scheme E also involves aptamer as sensing probe, but with slightly different design. Unlike the conventional linear conformation, aptamer used in this case includes a hairpin structure at one terminus.²³³ Only upon binding with target analyte, the stem part of hairpin opens up and hybridizes with

its complementary nucleotide sequence that has been pre-attached onto nano-amplifier surface. Via such mechanism, the aptamer-tethered fluorophore is incorporated in a much larger complex, so that the overall FP value increases significantly. LOD of this assay design for detecting ATP and thrombin can be as low as 20 pM and 0.3 pM respectively. They are more than six orders of magnitude lower than the control group without FP amplification.²³³

The assay design shown in scheme F is based on the competition between target analyte and its fluorophore-modified analogue for binding with sensing probe. In the initial state, the composite structure comprising fluorophore-modified target analogue, sensing probe and nano-amplifier demonstrates high FP value. Then following target addition, fluorophore-modified target analogue is displaced out of the composite. The degree of displacement depends on the similarity between target and its analogue, as well as their stoichiometry ratio. Along with the displacement, overall FP value of the system decreases. Though a large sensing probe such as antibody or other macromolecule might be adequate to induce considerable FP change upon target binding, inclusion of nano-amplifier can always further improve detection sensitivity and afford this FP-based assay the competitiveness in practical application.²²⁸

Besides the six configurations discussed above, there are many other AFP-based assays in literature that exploit much delicate designs.²³⁴ However, majority of them are relying on one or combination of the fundamental principles we have covered here (scheme A-F). Moreover, one may realize that FP-based assay shares numerous similarities with the FRET-based designs discussed in the previous section, since both (1) involve nanomaterials as either FP amplifier or fluorescence quencher, (2) are homogeneous assays that require no separation or washing steps, (3) are based on non-adulterated measurement. However, compared with FRET, FP-based assay design possesses additional advantage of higher reliability due to its ratio-based nature. This makes itself much more resistant to inner filter effect, dye photobleaching, nonspecific quenching, and non-uniform illumination problems. However, its downsides, such as requirement of expensive FP spectrometer and vulnerability to non-specific interaction with macromolecules, may balance against the advantage. Therefore, it is perhaps impossible to provide a universal guideline for the selection of assay principles and transducing elements for both AFP- and FRET-based biosensor designs, since it highly depends on the actual assay requirements including type of target analyte, sensitivity expectation, material availability, and potential applications.

Bio-barcode Assay (BCA)

Bio-barcode assay (BCA) was first demonstrated by Mirkin and co-workers in 2003.²³⁵ Strictly speaking, it is not a solution phase detection since washing and substrate-based target analysis may be involved.²³⁶ However, we prefer to include it in present review because its novel barcode amplification step occurs in solution and the signal transducing mechanism can vary from case to case, with some of them based in solution as well. More importantly, its detection sensitivity is extremely low, ranging from attomolar ($aM=10^{-18}$ M) to zeptomolar ($zM=10^{-21}$ M) level, which may provide additional opportunities for clinical diagnosis applications.

In typical BCA design, one copy of target analyte can be surrogated into multiple copies of DNA molecules called “barcode”.²³⁷ It is these barcode DNAs that undergo

quantitative analysis and give off detectable signals. Via such target-based amplification, much improved detection sensitivity can be achieved. And the improvement primarily depends on quantity ratio between target surrogate and target itself. In general, BCA is in hybrid form, involving two basic components. First is the magnetic microparticle (MMP) modified with capturing probes. Second is gold nanoparticle (AuNP) co-functionalized with another type of capturing probes and dsDNA molecules. This dsDNA is the hybridization product of barcode ssDNA and its complementary sequences that have been pre-tethered onto AuNP (see Figure 13). The two capture probes can recognize the same target, but at different epitopes. Therefore, sandwich-like structure can be formed and extracted out of the assaying solution by applying external magnetic field. The barcode DNA sequences are then discharged from AuNP surface via water or buffer washing at elevated temperature, and subject to analysis using various DNA analysis techniques. Following such protocol, the target analyte is successfully surrogated by multiple copies of ssDNA barcode sequences that can be detected with ultrahigh sensitivity.²³⁸

The first demonstrated example of BCA was for detecting protein molecule (e.g. prostate-specific antigen, PSA) using antibodies (anti-PSA-1 and anti-PSA-2) as capturing probes.²³⁵ The PSA target was firstly recognized by the anti-PSA-1 coated MMP, and then anti-PSA-2 coated AuNP probes were added in to form the sandwich-like complex (Figure 13). With scanometric barcode (DNA) analysis, LOD of 30 aM was achieved. And alternative DNA analysis using PCR allowed even lower LOD of 3 aM, six orders of magnitude lower than that of clinically accepted conventional assays. Some succeeding exploration further extends the BCA application in serum-based detection,²³⁹ as well as for some other target analytes including amyloid- β -derived diffusible ligands, HIV p24 Gag protein and bluetongue virus.²⁴⁰⁻²⁴² Furthermore, Liu and co-workers managed to transfer this bio-barcode design onto a single disposable chip device.²⁴³ LOD of 500 aM was successfully demonstrated using PSA as model target.

With slight modification, BCA can also be utilized for DNA detection while attaining its ultrahigh sensitivity. In the modified design, two types of ssDNA sequences replaced the two antibody capturing probes on MMP and AuNP, respectively.²⁴⁴ Each sequence was perfectly complementary with half of the desired target analyte. Therefore, DNA hybridization catalysed the sandwich structure formation. Achieved LOD of 500 zeptomolar ($z\text{M}=10^{-21}$ M) using scanometric technique was equivalent to about 10 copies of DNA molecules in the entire 30 μL sample volume.²⁴⁴ Such detection sensitivity was comparable with that of PCR. Similar with PCR, this BCA design is implemented in homogeneous solution as well. It therefore allows people to utilize high concentration of AuNP and MMP probes to push the reaction equilibrium toward the formation of sandwich complex and to enhance the target binding kinetics.

In spite of all the merits and corresponding examples above, BCA assays suffer from numerous drawbacks as well. For instance, it requires many experimental and analytical steps, especially the synthetically demanding scanometric or PCR techniques for barcode analysis, which make such assay very tedious and rather costly. Also, in the scanometric analysis, it is difficult to achieve consistent and complete barcode loading on the surface-support strands via hybridization. Such inefficiency, to large extent, increases the experimental variability. Moreover, the dose response, defined as net amount of

generated signals for unit increase of target concentration, is relatively low. In other words, a large increase in target concentration can only lead to limited signal increment. In order to circumvent these downsides, intensive efforts have been devoted in recent years to simplify the assay process and also explore other convenient readout possibilities. Up to date, several new versions of BCA assays have been devised as shown in later discussion, inheriting the ultrahigh sensitivity from the very original design but averting some of the critical shortcomings.

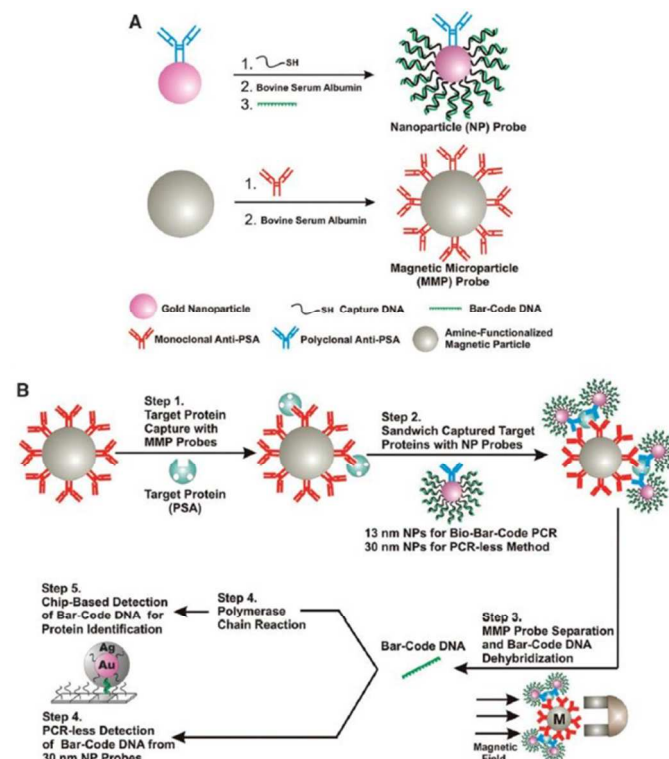


Figure 13 The bio-barcode assay method. (A) Illustration of the two key components: AuNP modified with sensing probe I and barcode DNA; MMP functionalized with sensing probe II; (B) Typical bio-barcode assay procedures for PSA detection. Reprinted with permission from ref. 235, © 2003 American Association for the Advancement of Science.

Following the bio-barcode assay invention, Mirkin and co-workers reported another new AuNP probe for BCA that only required modification with single type of DNA, instead of three in the original design (including target-specific probe strand, thiolated barcode-capturing strand and barcode itself).^{245,246} The new probing DNA was single stranded with thiol-labels for AuNP tethering. It performs as target-specific sensing probe, as well as the barcode oligonucleotide. After target crosslinking and magnetic extraction, the thiolated ssDNA can be discharged from AuNP using dithiothreitol (DTT), followed by scanometric analysis as usual. Experiment showed a successful detection of the mock mRNA target with 7 aM LOD at favourable conditions. Compared with the original design, present example exhibits simplified synthetic process and enhanced quantitative capability. However, its dose response is rather shallow, with 10,000-fold increase in target concentration leading to only <10 times of signal increase. Müller and co-workers demonstrated the possibility of thousand-fold increase in dose response without sacrificing the

detection sensitivity.²⁴⁷ Such effort makes the BCA principle more analytically useful, as more accurate calibration curve can be obtained with this improved dose response.

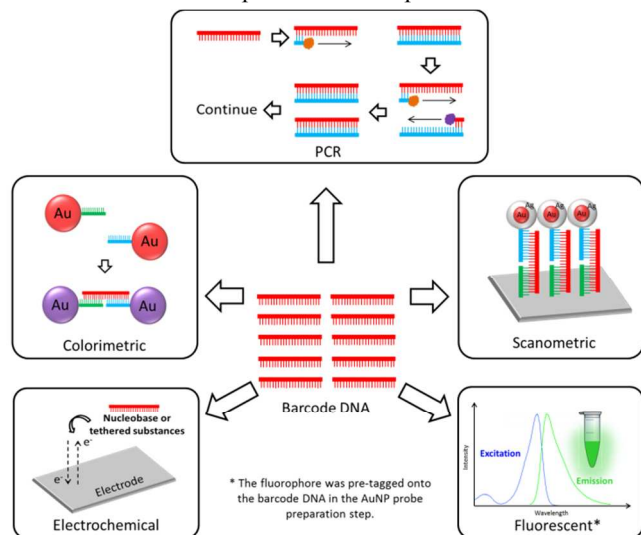


Figure 14 Various techniques for analysing the barcode DNA after discharged from the AuNP probe.

Instead of scanometric and PCR techniques, many alternative methods for barcode DNA analysis have been made available and demonstrated several competitive edges (

Figure 14). For example, Groves and co-workers reported a colorimetric-based BCA design for ultrasensitive detection of cytokine (e.g. interleukin-2).^{248,249} AuNP in conventional design was replaced with porous silica particle of 3 μm diameter. Its large size and high porosity permitted millions of barcode DNAs attached on surface. After magnetic extraction and barcode discharging, the single-stranded barcode sequence was analysed using ssDNA functionalized AuNP. Barcode DNA herein can crosslink the AuNP and induce colour change from red to blue (or purple). Quantitative analysis of AuNP aggregation was accomplished using Thin-Layer Chromatography (TLC) plate, with 30 aM LOD achieved both in buffer and in human serum samples. Such colorimetric assay design might be of great clinical application for diagnosis of Alzheimer's disease, as cytokines have been widely considered as the Alzheimer biomarker with maximum allowable concentration around 100 aM.²⁴⁰ In addition, Oh and some others developed fluorescence-based BCA by attaching luminescent tags onto barcode DNA.²⁵⁰⁻²⁵⁴ Therefore, the barcode could be directly quantified by measuring the fluorescence emission intensity. Such fluorescence-based design had been successfully demonstrated for detecting various bio-targets, including PSA,²⁵⁰ DNA,²⁵¹ avian influenza virus,²⁵² and Salmonella enterica serovar Enteritidis.²⁵³

The electrochemical read-out is another alternative of particular attention.²⁵⁵⁻²⁶⁰ However, the detailed assay design differs from case to case. In the first, all the procedures were similar with the conventional assay, except for the barcode analysis step. Barcode sequences in this case were specially designed, either poly-A or poly-G. They underwent hydrolysis in heated H_2SO_4 environment. The obtained nucleobases were then electrochemically detected by virtue of their respectively redox properties.^{255,256} In the second case, barcode DNA was

labelled by some tracers like PbS or CdS.²⁵⁹ These tracers would be released by appropriate treatment and detected electrochemically using screen-printed carbon electrode. In the third case, the functionalized AuNP composite was immobilized onto a bulky substrate. The AuNP-tethered DNA was hybridized by PbSNP-labelled barcode DNA. Released Pb^{2+} was detected through differential pulse anodic stripping voltammetry.²⁵⁷ The fourth case resembled the third. Only difference was, instead of PbSNP, the barcode sequences were bound with $[\text{Ru}(\text{NH}_3)_6]^{3+}$. Such Ru-based complex could produce detectable chronocoulometric signals at appropriate condition.²⁵⁸ However, as mentioned at the beginning of this section, BCA is not purely solution phase, especially the third and fourth cases above, in which flat substrate is involved. They are included here, only for the purpose of providing a complete overview of this ultrasensitive principle.

In addition, Hill *et al.* reported another novel BCA design for detecting double-stranded genomic DNA from *Bacillus subtilis*.²⁶¹ The functionalized MMP- and AuNP-based composites were prepared as usual. Critical step in this new design was the dehybridization of target dsDNA and the utilization of blocker oligonucleotides. These blockers were to bound with specific regions of the dehybridized target DNA upon cooling and prevented it from re-hybridization. Therefore, the produced ssDNA sequences were available as pseudo-target, transforming the dsDNA detection task into ssDNA based one. Multiplexed target detection, such as various protein cancer markers,²⁶² different oligonucleotides^{256,263} and gene sequences,²⁵⁹ has been realized as well using BCA principles with the same scheme but different sensing probes.

Compared with the FRET or AFP-based assays, it is the ultrahigh detection sensitivity that makes the bio-barcode principle much outstanding among various assay designs. It offers great potential for clinical application of biological maker identification and therapeutic purposes. More importantly, when it becomes possible to detect specific target(s) at extremely low level, detection sensitivity is no longer the driving force of the research. Instead, it will be the time to answer questions of how this technology can be applied and benefit human community. In modern clinical practices, a cut-off concentration is usually set for specific biomarker(s) to differentiate the health and disease situations. Such concentration is limited by current technology. With the application of ultrasensitive bio-barcode assay, that cut-off concentration can be significantly lowered, which not only contributes to the even earlier diagnostics of associated diseases, but also provides a more informative target monitoring approach that can greatly assist clinicians in their examination on patients.

Chemiluminescence (CL)

Chemiluminescence (CL), as inferred by its name, is the luminescent emission from chemical reactions. Perhaps the most well-known example for biosensor application is the substrate oxidation catalysed by horseradish peroxidase (HRP),²⁶⁴⁻²⁶⁶ which has been intensively explored in the conventional microplate ELISA. Intrinsically, CL can only take charge of the signal transducing process, leaving target recognition open to any of the aforementioned mechanisms, including DNA hybridization, antibody-antigen binding, and aptamer-target interaction. For example, by exploiting DNA hybridization, Fan and co-workers²⁶⁴ reported a magnetic separation-based CL sensor with pM sensitivity (

Figure 15). The design comprised two main components: ssDNA functionalized magnetic particle (MP) and AuNP-based composite. The AuNP herein is triply functionalized with ssDNA, HRP and BSA as sensing probe, signal transducer and surface blocker, respectively. Added ssDNA target is able to crosslink the two components by hybridizing with the two probes. Formed sandwich-like structure is then magnetically extracted out of solution and undergoes optical analysis in a medium that contains HRP-catalysing substrate. In other words, only in the presence of target ssDNA, HRP could be isolated from the assaying solution and catalyse the substrate oxidation for optical signals generation. Target of 100 pM concentration showed naked eye detectable colour contrast. Instrument-assisted reading further lowered the LOD down to 1.0 pM. Moreover, tethering secondary AuNP-composite onto the MP-AuNP complex could further increase the HRP loading density, which led to another 10-fold improvement in detection sensitivity.²⁶⁷

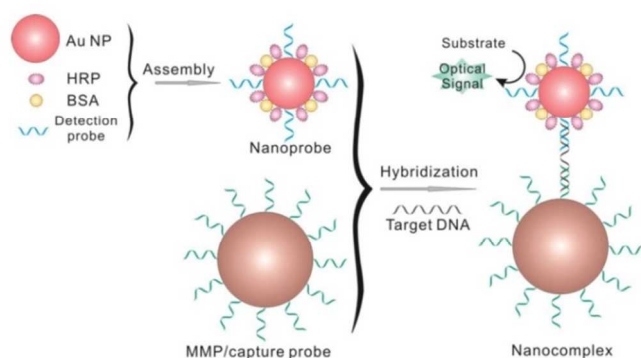


Figure 15 The magnetic bead-AuNP based chemiluminescence biosensor for ssDNA detection. Added target ssDNA is able to crosslink the MMP and AuNP composites, facilitating the subsequent magnetic extraction of the sandwich-like complex out of assaying solution and further optical signal generation by reacting with oxidation substrate. Reproduced with permission from ref. 264, © 2008 WILEY.

Recently, many nanomaterials (e.g. GO, CNT and their various derivatives) are found to exhibit peroxidase-like activity, which provides additional opportunities of designing CL-based biosensor. Yang and co-workers reported a solution phase sensor for PSA detection using magnetic particle (MP) and GO.²⁶⁸ MP was functionalized with one type of PSA-specific antibody as sensing probe and GO was functionalized with another type. In PSA presence, sandwich-like structure was formed and magnetically isolated from assay solution. Therefore, target PSA concentration was translated into the amount of extracted GO. Such GO was further employed to catalyse hydroquinone oxidation reaction by H_2O_2 . The colour change could be clearly observed for PSA concentrations of above and below 4 ng/mL, which was the cut-off value to distinguish the people possibly with prostate cancer from the healthy. As another example, Qu and his colleagues developed a highly sensitive (1 μ M LOD) solution phase copper ion (Cu^{2+}) sensor, using the enhanced peroxidase-like activity of MCNT.²⁶⁹ In principle, azide-functionalized magnetic silica nanoparticles can conjugate with acetylene-functionalized MWNT in presence of Cu^{2+} and sodium ascorbate. The obtained hybrid composite exhibited much higher peroxidase-like activity than MWNT alone, which was evident from the faster colour change upon addition of H_2O_2 and reaction

substrate (TMB). As control, no detectable signals could be seen in absence of Cu^{2+} target.

Moreover, nanomaterial's peroxidase-like activity can work collaboratively with its other characteristics, thereby providing much more versatile design possibilities for the CL-based biosensor construction. By exploiting the peroxidase-like activity of graphene-AuNP interface and the different binding affinities of ssDNA/dsDNA towards the aromatic surface, Quan and co-workers proposed a novel sensing scheme that could be used for diverse applications, including detection of DNA, sensing of protein-aptamer interaction and monitoring of enzymatic DNA cleavage.²⁷⁰ The peroxidase-like activity was found at graphene-AuNP interface, although graphene or AuNP alone showed little catalysing capability. Due to the strong affinity, added ssDNA or aptamer would adsorb onto graphene and prevent the peroxidase substrate from diffusing to and binding with the active interface. Catalytic reaction was therefore largely retarded. Introducing target analytes (e.g. complementary DNA sequence, aptamer-specific substrate or DNA enzymes) could liberate ssDNA from graphene surface in respective manners and make the graphene-AuNP interface accessible for peroxidase substrate. Catalytic reaction was switched on and started producing luminescent signals.

In some other special cases, nanomaterial was not contributing to the peroxidase-like activity at all, but solely performing as sensing probe or signal amplifier. Dong and co-workers reported a novel colorimetric assay for detecting ssDNA target and single-nucleotide polymorphism, using hemin-graphene hybrid assembly.²⁷¹ In the assembly, it was the hemin molecule that exhibited peroxidase-like activity. Graphene only performed as precipitation inducer in the design. In presence of dsDNA, hemin-graphene complex was easily precipitated by adding in electrolyte, whereas mixture of the complex and ssDNA showed no precipitation under identical ionic strength. As following, the un-precipitated solution was utilized to catalyse CL reactions and produce detectable signals. Experimentally, the solution absorbance value decreased linearly with the concentration of target ssDNA up to 100 nM. LOD was reported as 2 nM based on the 3 δ rule.

The last example to present in this section is rather complicated, involving mechanisms of CL, fluorescence energy transfer, aptamer-target interaction, as well as enzymatic digestion (see Figure 16).²⁶⁶ The system comprised FAM-labelled DNA functionalized-AuNP, hairpin-structured aptamer, exonuclease III (Exo III) and luminol- H_2O_2 -HRP complex. In absence of the target analyte (e.g. thrombin), the produced CL energy from CL was transferred to FAM via chemiluminescence resonance energy transfer (CRET). Such energy was then quenched by AuNP via FRET due to FAM-AuNP proximity. However, in presence of target, the hairpin-structured aptamer would open up and form aptamer-target complex with an oligonucleotide tail at 5'-end. The tail could hybridize with the DNA sequence which was pre-attached onto AuNP at one end and pre-modified with FAM at the other. Formed dsDNA then activated selective cleavage of the FAM-labelled DNA sequences by Exo III, liberating FAM and aptamer-target complex back into solution. The free FAM now demonstrated fluorescence via aforementioned CRET mechanism. The released aptamer-target complex could hybridize with another FAM-labelled DNA, and initiated the hybridization-digestion-release cycle all over again. Ultrahigh sensitivity (2 fM LOD) of present design was reported, benefit from the cyclic signal amplification mechanism (see Figure 16).

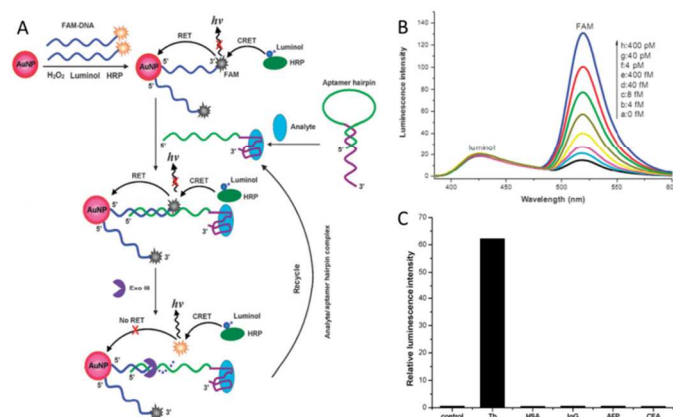


Figure 16 (a) Schematic illustration of the amplified CRET aptasensor based on bi-resonance energy transfer, (b) The CL spectra of the CRET aptasensor for analysing target thrombin at different concentrations, (c) Illustration of detection selectivity of the fabricated CRET aptasensor. Reproduced with permission from ref. 266, © 2012 Royal Society of Chemistry.

Design Principles Comparison

After going through all the design principles of the dual-transducer biosensors covered in this review, it is time to look back at the two questions we posed in the introduction, and set about answering them.

What are the additional opportunities that nanomaterial based dual-transducer biosensors can provide relative to the single nanomaterial based counterpart?

First and foremost, the combined use of dual transducing elements contributes to the well-enhanced design versatility. In general, each type of nanomaterial possesses several fascinating and unique characteristics. With single nanomaterial transducer, only the individual feature of that particular nanomaterial or interaction among neighbouring nanomaterials of the same identity can be employed, which largely restricts the design flexibility and versatility. On the other hand, in the dual-transducer design, utilization of different types of nanomaterials or combining nanomaterial with other transducing elements can significantly broaden the spectrum of possible design configurations. Take the metal nanoparticles as examples, when the AuNP or AgNP alone is used as transducing element, the majority of the reported assays are based on aggregation-induced colour change that arises from the LSPR band shift. In comparison, in the dual-transducer designs illustrated above, the AuNP or AgNP exhibits various roles, including fluorescence quencher in FRET,^{154,164,168,175,181-183} fluorescence enhancer,⁷¹ polarization amplifier in AFP,²²⁸⁻²³⁰ probe carrier in both BCA and CL.^{235,239,240,244,245,264,267} Nowadays, biosensors in different fields have different requirements and restrictions. For example, in the initial stage of drug screening, assay designs with low cost and easy operation are preferred, in order to screen the drug candidates in a high throughput and rapid manner. However, in cancer diagnosis, ultrahigh sensitivity and selectivity are always the most primary concerns, overstepping all the other factors like cost-effectiveness and portability. Hence, with the additional design possibilities, we can always select the most suitable one that best accommodates the practical requirements.

Moreover, the idea of enhancing design versatility can be further extended to the signal transducing step, such as the dual-signal based (both fluorescent and colorimetric) design for Hg²⁺ detection.¹⁶² With dual transducing elements, biosensors can be constructed in a way that multiple signals are generated by a single target via different mechanisms. These signals can verify, support and reinforce each other, resulting in improved and more reliable sensing capability. The multiplexed detection discussed in the FRET and BCA sections of this review is another example of sensor design with versatility, in which various targets are mixed with a single assay kit and generate discrete signals for respective target.^{108,111,172,182,211,256,259,262,263} Such design not only reduces the assaying time and cost, but also makes the sample comparison feasible, reproducible and much reliable as well.

Second, in terms of performance, it is impractical to claim superiority for either the single nanomaterial based or the dual-transducer based schemes because similar LOD in pM to nM range are observed for both. However, it is worth highlighting that the dual-transducer design can always employ the single-transducer sensing principle, but possibly equipped with additional signal amplification mechanism to further enhance detection sensitivity. For instance, one of the modified BCA designs was based on ssDNA-induced AuNP crosslinking and subsequent solution colour change. What makes it outstanding is that, those ssDNA sequences are not the real target analytes. Instead, they are merely barcode surrogates released from the target-induced sandwich-like structure. With such amplification mechanism, LOD of aM (10^{-18} M) level was demonstrated, significantly lower than those from direct target-induced aggregation designs. Nevertheless, it should also be noted that, the dual-transducer based biosensors are in general more synthetically demanding, because multitude bio-functionalization procedures may be required for different transducing elements. This will jeopardize the cost-effectiveness and convenience of the dual-transducer biosensors in practical application and further possible commercialization.

What are the advantages and disadvantages for each of the four discussed dual-transducer biosensing principles?

Comparison of the four design principles is summarized in Figure 17 in terms of detection sensitivity, selectivity, versatility, cost-effectiveness, design robustness, and portability. According to Giljohann *et al.*,² these six factors are the drivers for biodiagnostic development, which we believe can also be used for assessing the respective biosensor designs. For each factor, four levels are set (from 1 to 4), with 1 being the worst and 4 being the best. These numbers are arbitrarily assigned based on the comparative merits of each principle. We herein borrow the concept of "Holland Vocational Interest Test" to illustrate the comparison result. The plot shown in Figure 17 clearly indicates merits and demerits for each principle, with overall performance well reflected from the hexagon shape, area and orientation.

Detection Sensitivity There is no doubt that bio-barcode assay (BCA) provides the most sensitive detection (assignment of level 4) due to its target-based signal amplification and availability of ultrasensitive DNA analysis techniques. The zeptomolar ($zM=10^{-21}$ M) LOD for ssDNA target is comparable with PCR technique.²⁴⁴ Such sensitivity has not been achieved so far for the other three principles, in which most of the LOD only range from picomolar ($pM=10^{-12}$ M) to micromolar

($\mu\text{M}=10^{-6}$ M), depending on the actual situation. Therefore, level 2 is arbitrarily assigned.

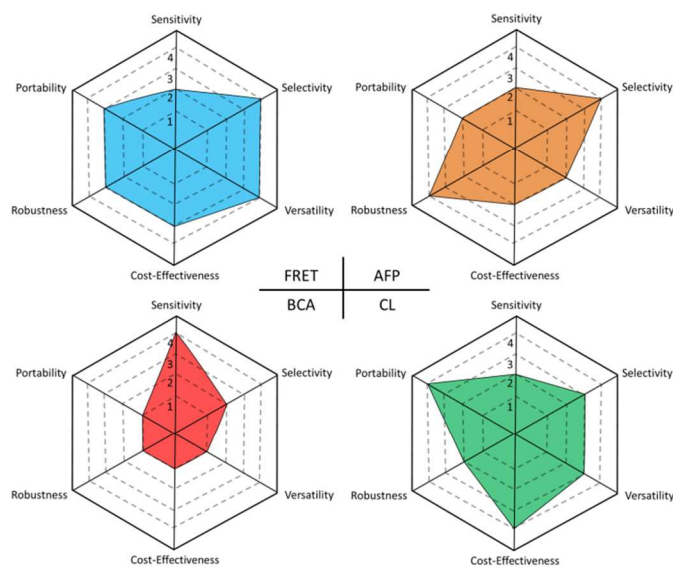


Figure 17 Comparison of the four dual-transducer design principles: Förster Resonance Energy Transfer (FRET), Amplified Fluorescence Polarization (AFP), Bio-barcode Assays (BCA) and Chemiluminescence (CL).

Detection Selectivity Biosensor selectivity is primarily determined by reaction specificity of the utilized sensing probe. Common probe materials, such as ssDNA, aptamer, antibody, bio-reactive ligands, have been well explored for the four principles. Given a particular sensing probe, detection selectivity also highly depends on the transducing mechanism (direct transducing vs. indirect transducing). Herein, direct transducing means it is the bio-recognition process that directly leads to signal generation, whereas indirect transducing refers to the case in which a third mechanism is required to link the bio-recognition and signal generation steps. Take AuNP-based colorimetric assay as example. The crosslinking design is direct transducing because target-probe hybridization directly leads to solution colour change. However, the non-crosslinking design is indirect transducing, since following dsDNA formation, it is the van der Waals interaction that brings individual particle into aggregation.

It is not difficult to see that detection selectivity of direct transducing is superior to the indirect scheme, because the latter scenario is more vulnerable to environmental interferences. Concreting such concept to the four principles, AFP and FRET assays are direct transducing, hence exhibiting better selectivity than the CL-based assays, majority of which are indirect transducing. BCA is perhaps the least selective among the four, mainly because its target recognition and signal generation are well separated by multiple procedures in between. Therefore, the four principles should follow the selectivity merit order of $\text{FRET} \approx \text{AFP}$ (level 4) > CL (level 3) > BCA (level 2). In addition, it is worth highlighting that most of the reported assays involving non-specific adsorption on acceptor "A" (e.g., Figure 6 B and D, Figure 8 C and D, Figure 9 B, Figure 12 C and D) under FRET and AFP principles are only carried out in biological buffers (e.g., PBS,^{109,169,170,180,193} Tris-HCl,^{162,166,177} HEPES,¹⁷¹ and MOPS¹⁶¹) where no or limited interfering

molecules are present as in real biological matrix (e.g., serum or urine). Therefore, the selectivity of such designs in complex environments remains unclear. However, aptamer, as a highly specific sensing probe, has demonstrated its advantageous edge of binding to the target analyte in complex samples like serum²³³ or living cells.^{164,165} This renders the aptasensor family high potential for real life clinical applications.

Versatility In FRET, the donor and acceptor can be selected from a large pool of possible candidates (e.g., QD, UCNP, organic dye, CD for both donor and acceptor; AuNP, GO, CNT for acceptor). Hence, the FRET biosensors can be designed in a much more versatile manner to address those practical requirements and constraints. In CL-based assays, although only a few nanomaterials (e.g. AuNP, GO, CNT) has been employed, not as many as in FRET, their roles in the actual designs vary from case to case, including probe carrier, fluorescence quencher, enzyme mimics and precipitation inducer. With these wide-ranged roles, corresponding CL-based design can be flexible and versatile as well. Nonetheless, in AFP the roles that nanomaterial plays are rather limited, simply fluorescence polarization amplifier which magnifies the complex size change before and after target binding. As for BCA, most designs follow the same configuration of sandwich-like structure, in which nanomaterial roles are merely restricted to barcode carrier. Therefore, the versatility merit should follow the order of FRET (level 4) > CL (level 3) > AFP (level 2) > BCA (level 1).

Cost-Effectiveness In general, cost of biosensor includes two components: signal readout device and biosynthetic construction. The FRET and AFP assays demonstrate similar synthetic procedures, including transducer bio-modification and target recognition. However, the AFP design requires additional apparatus for fluorescence polarization measurement. As for the CL-based sensors, actual design configurations vary from case to case, depending on the utilized nanomaterial and detailed sensing mechanism; but its cost is normally lower than the FRET or AFP because it does not require any photo-excitation and only generate solution colour change as read-out signal. Such signal is detectable by naked eyes. Even if using UV-Vis to quantify such signal, UV-Vis spectrometer is usually much cheaper than the fluorescence spectrometer. The BCA design is perhaps the most cost-demanding among the four, because of the delicate ultrasensitive DNA analysis instruments. In addition, cost on the consumed reagents and the time required (how manpower is paid for) per assay running should also be included when evaluating cost-effectiveness of certain biosensor design. As for the four design principles covered here, it is difficult to compare their reagent cost, simply because the type and quantity of consumed reagents are highly dependent on the desired target analyst and price can vary significantly. However, when it comes to the man-hour cost required per assay, there is no doubt that BCA is the most time consuming, as multiple washing and hybridization steps, as well as post DNA sequence analysis, are involved. For the other three, no clear distinctions can be drawn. Therefore, the overall merit order for cost-effectiveness (mainly according to instrument cost) follows CL (level 4) > FRET (level 3) > AFP (Level 2) > BCA (level 1).

Robustness Biosensor robustness could mean the reliability of sensor design in different ambient conditions. No much data in this aspect has been reported, because the majority of the demonstrated examples are still in lab-testing stage with optimized experimental conditions. However, to the best of our knowledge, we would rank AFP-based design the highest

robustness (level 4) because it relies on the ratio of fluorescence intensities in two perpendicular directions. Compared with the assays using absolute fluorescence intensity (e.g. CL), such ratio-based measurement are more resistant to possible interferences, such as photobleaching and non-uniform excitation. In field application, even if absolute intensity changes, the ratio can stay intact. This can certainly enhance the robustness of such design. The ratio-based readout can also be applied to FRET biosensors, simply by comparing the intensities of donor and acceptor fluorescence. However, we can only assign level 3 to FRET, because the nominator and denominator of the ratio come from two different fluorescent components (donor and acceptor), and each component could be subject to environmental interferences in different ways and degrees. This makes it less robust compared with the AFP concept, where the nominator and denominator both come from single fluorescent agent (along two perpendicular directions). BCA is probably the least robust due to its multitude assay steps (level 1). Therefore, overall merit order of design robustness is AFP (level 4) > FRET (level 3) > CL (level 2) > BCA (level 1).

Portability If excluding the signal read-out device, FRET, AFP and CL principles should demonstrate similar merit of portability because they are all based on mix-and-measure protocol. Comparatively, BCA is more complicated due to its multitude analytical steps. Nonetheless, if taking the read-out device into consideration, FRET is advantageous to AFP simply because AFP requires additional fluorescence polarizer apparatus. CL is perhaps the most portable design among the four because its signal of colour change allows naked eye based detection. Even though UV-Vis absorption might be required to quantify the generated colour change, current technology allows fabrication of miniaturized UV-Vis spectrometer, which can be much smaller in size than fluorescence spectrometers. Therefore, we assign the portability merit in the order of CL (level 4) > FRET (level 3) > AFP (level 2) > BCA (level 1).

Summary and Outlook

The incorporation of nanomaterial transducer with collaborative transducing elements opens up a new era for further development of novel biosensors of detecting a broad range of target analytes. With the assistance of representative examples from Förster Resonance Energy Transfer (FRET), Amplified Fluorescence Polarization (AFP), Bio-barcode Assay (BCA) and Chemiluminescence (CL) principles, we have demonstrated the basic design rules and performances of the dual-transducer based biosensors. Within this review, we did not intend to cover the entire literature in this research field. Even within the four principles, we only include representative papers with significant breakthroughs either in sensing performance or design concept. We hope this review can serve the role of summarizing recent advances in the research field, as well as stimulating more interests in the dual-transducer based biosensor development.

In spite of the remarkable progresses achieved, there still exist several challenges (we would call opportunities) that could perform as guidelines for further development in this field. First and foremost, incorporation of inorganic nanomaterials introduces heterogeneous interfaces in the homogeneous bio-system. This may lead to slow binding kinetics, low recognition efficiency, and some more severe problems associated with nanotoxicity.^{272,273} Additional efforts

are therefore required to resolve this concern. Second, most efforts on bioassay development are devoted to the improvement of target recognition and signal amplification steps, but very limited attention is focused on the post-data processing. Sometimes proper data acquisition (e.g. kinetic monitoring) and in-depth data analysis (e.g. pattern recognition) are able to enhance the sensor performance and provide adequate information for target identification and quantification.^{274,275} Third, near infrared (NIR) detection have been underexplored, but deserves particular attention, because the NIR signal can penetrate through complex biological samples, such as whole blood, serum and urine. For demonstration of concept, the majority of the reported assays are based in biological buffer, or even DI water; but ultimately target detection should be conducted in body fluid or *in vivo*, which renders NIR-based assays the particular importance and significance. Last but not least, translation of various assay designs from laboratory based proof-of-concept to commercial products in marketplace requires long-term endeavours from both academic and industry communities, in order to promote the landscape of disease diagnosis, healthcare, and environment monitoring to the next level.

Acknowledgements

SuX would like to acknowledge the Agency for Science, Technology and Research (A*STAR), Singapore, for the financial support of JCO 14302FG096 and ETPL/13-R15GAP-0011.

Notes

^a Institute of Materials Research and Engineering, Agency for Science, Technology and Research (A*STAR), 3 Research Link, Singapore 117602

^b Department of Chemistry, University of Illinois at Urbana-Champaign, Urbana, Illinois 61801, United States

* Corresponding Author: xd-su@imre.a-star.edu.sg

References

1. P. Alivisatos, *Nat. Biotechnol.*, 2003, 22, 47.
2. D. A. Giljohann, C. A. Mirkin, *Nature*, 2009, 462, 461.
3. D. F. Moyano, V. M. Rotello, *Langmuir*, 2011, 27, 10376.
4. E. Katz, I. Willner, *Angew. Chem. Int. Ed.*, 2004, 43, 6042.
5. D. Alili, M. M. Stevens, *Chem. Soc. Rev.*, 2010, 39, 3358.
6. D. F. Moyano, V. M. Rotello, *Langmuir*, 2011, 27, 10376.
7. R. Wilson, *Chem. Soc. Rev.*, 2008, 37, 2028.
8. W. Zhao, M. A. Brook, Y. Li, *ChemBioChem*, 2008, 9, 2363.
9. Z. Wang, Y. Lu, *J. Mater. Chem.*, 2009, 19, 1788.
10. Y.-W. Lin, C.-W. Liu, H.-T. Chang, *Anal. Methods*, 2009, 1, 14.
11. W. Zhong, *Anal. Bioanal. Chem.*, 2009, 394, 47.
12. S. Song, Y. Qin, Y. He, Q. Huang, C. Fan, H.-Y. Chen, *Chem. Soc. Rev.*, 2010, 39, 4234.
13. W. R. Algar, K. Susumu, J. B. Delehanty, I. L. Medintz, *Anal. Chem.*, 2011, 83, 8826.
14. X. Cao, Y. Ye, S. Liu, *Anal. Biochem.*, 2011, 417, 1.
15. D. Liu, Z. Wang, X. Jiang, *Nanoscale*, 2011, 3, 1421.
16. Y.-W. Lin, C.-C. Huang, H.-T. Chang, *Analyst*, 2011, 136, 863.
17. V. K. K. Upadhyayula, *Analytica Chimica Acta*, 2012, 715, 1.
18. L. M. Zanolli, R. D'Agata, G. Spato, *Anal. Bioanal. Chem.*, 2012, 402, 1759.
19. H. Jans, Q. Huo, *Chem. Soc. Rev.*, 2012, 41, 2849.

- 1
2
3
4
5
6
7
8
9
10
11
12
13
14
15
16
17
18
19
20
21
22
23
24
25
26
27
28
29
30
31
32
33
34
35
36
37
38
39
40
41
42
43
44
45
46
47
48
49
50
51
52
53
54
55
56
57
58
59
60
20. K. Saha, S. S. Agasti, C. Kim, X. Li, V. M. Rotello, *Chem. Rev.*, 2012, 112, 2739.
21. J. Li, J.-J. Zhu, *Analyst*, 2013, 138, 2506.
22. Y. Wang, R. Hu, G. Lin, I. Roy, K.-T. Yong, *ACS Appl. Mater. Interfaces*, 2013, 5, 2786.
23. J. Wang, X. Qu, *Nanoscale*, 2013, 5, 3589.
24. H. Jang, J. Lee, D.-H. Min, *J. Mater. Chem. B*, 2014, 2, 2452.
25. J.-J. Xu, W.-W. Zhao, S. Song, C. Fan, H.-Y. Chen, *Chem. Soc. Rev.*, 2014, 43, 1601.
26. L.-C. Ho, C.-W. Wang, P. Roy, H.-T. Chang, *J. Chin. Chem. Soc.*, 2014, 61, 163.
27. P.-C. Chen, P. Roy, L.-Y. Chen, R. Ravindranath, H.-T. Chang, *Part. Part. Syst. Charact.*, 2014, DOI: 10.1002/ppsc.201400043.
28. W. Deng, E. M. Goldys, *Analyst*, 2014, 139, 6321.
29. J. Wang, *Analyst*, 2005, 130, 421.
30. Y. Yonemori, E. Takahashi, H. Ren, T. Hayashi, H. Endo, *Analytica Chimica Acta*, 2009, 633, 90.
31. R. Rossetti, S. Nakahara, L. E. Brus, *J. Chem. Phys.*, 1983, 79, 1086.
32. L. Shao, Y. Gao, F. Yan, *Sensors*, 2011, 11, 11736.
33. F. A. Esteve-Turrillas, A. Abad-Fuentes, *Biosens. Bioelectron.*, 2013, 41, 12.
34. P. Reiss, M. Protière, L. Li, *small*, 2009, 5, 154.
35. D. A. Hines, P. V. Kamat, *ACS Appl. Mater. Interfaces*, 2014, 6, 3041.
36. I. L. Medintz, H. Mattoussi, *Phys. Chem. Chem. Phys.*, 2009, 11, 17.
37. Z. Jin, N. Hildebrandt, *Trends Biotechnol.*, 2012, 30, 394.
38. W. C. W. Chan, S. Nie, *Science*, 1998, 281, 2016.
39. M. B. Jr., M. Moronne, P. Gin, S. Weiss, A. P. Alivisatos, *Science*, 1998, 281, 2013.
40. C. Luccardini, C. Tribet, F. Vial, V. Marchi-Artzner, M. Dahan, *Langmuir*, 2006, 22, 2304.
41. K. Susumu, H. T. Uyeda, I. L. Medintz, T. Pons, J. B. Delehanty, H. Mattoussi, *J. Am. Chem. Soc.*, 2007, 129, 13987.
42. E. Gravel, C. Tanguy, E. Cassette, T. Pons, F. Knittel, N. Bernards, A. Garofalakis, F. Ducongé, B. Dubertret, E. Doris, *Chem. Sci.*, 2013, 4, 411.
43. N. Chen, Y. He, Y. Su, X. Li, Q. Huang, H. Wang, X. Zhang, R. Tai, C. Fan, *Biomaterials*, 2012, 33, 1238.
44. M. Bottrill, M. Green, *Chem. Commun.*, 2011, 47, 7039.
45. C. Kirchner, T. Liedl, S. Kuder, T. Pellegrino, A. M. Javier, H. E. Gaub, S. Stolzle, N. Fertig, W. J. Parak, *Nano Lett.*, 2005, 5, 331.
46. F. Chen, D. Gerion, *Nano Lett.*, 2004, 4, 1827.
47. S. T. Selvan, T. T. Tan, J. Y. Ying, *Adv. Mater.*, 2005, 17, 1620.
48. F. M. Winnik, D. Maysinger, *Acc. Chem. Res.*, 2013, 46, 672.
49. K.-T. Yong, H. Ding, I. Roy, W.-C. Law, E. J. Bergey, A. Maitra, P. N. Prasad, *ACS Nano*, 2009, 3, 502.
50. S. Kim, H. Mohseni, M. Erdtmann, E. Michel, C. Jelen, M. Razeghi, *Appl. Phys. Lett.*, 1998, 73, 963.
51. J.-H. Park, L. Gu, G. v. Maltzahn, E. Ruoslahti, S. N. Bhatia, M. J. Sailor, *Nat. Mater.*, 2009, 8, 331.
52. F. Erogbogbo, K.-T. Yong, I. Roy, G. Xu, P. N. Prasad, M. T. Swihart, *ACS Nano*, 2008, 2, 873.
53. E. C. Dreaden, A. M. Alkilany, X. Huang, C. J. Murphy, M. A. El-Sayed, *Chem. Soc. Rev.*, 2012, 41, 2740.
54. G. Frens, *Nature Phys. Sci.*, 1973, 241, 20.
55. C. A. Mirkin, R. L. Letsinger, R. C. Mucic, J. J. Storhoff, *Nature*, 1996, 382, 607.
56. Y. N. Tan, K. H. Lee, X. Su, *RSC Adv.*, 2013, 3, 21604.
57. Y. N. Tan, X. Su, Y. Zhu, J. Y. Lee, *ACS Nano*, 2010, 4, 5101.
58. X. Xie, R. Deng, F. Liu, W. Xu, S. F. Y. Li, X. Liu, *Anal. Methods*, 2013, 5, 1116.
59. X. Su, R. Kanjanawarut, *ACS Nano*, 2009, 3, 2751.
60. R. Kanjanawarut, X. Su, *Anal. Chem.*, 2009, 81, 6122.
61. Y. N. Tan, X. Su, E. T. Liu, J. S. Thomsen, *Anal. Chem.*, 2010, 82, 2759.
62. Y. N. Tan, K. H. Lee, X. Su, *Anal. Chem.*, 2011, 83, 4251.
63. X. Xie, W. Xu, T. Li, X. Liu, *small*, 2011, 7, 1393.
64. Z. Wang, J. H. Lee, Y. Lu, *Adv. Mater.*, 2008, 20, 3263.
65. J. Liu, Y. Lu, *J. Am. Chem. Soc.*, 2003, 125, 6642.
66. J. Liu, Y. Lu, *J. Am. Chem. Soc.*, 2004, 126, 12298.
67. J. Liu, Y. Lu, *J. Am. Chem. Soc.*, 2005, 127, 12677.
68. J. H. Lee, Z. Wang, J. Liu, Y. Lu, *J. Am. Chem. Soc.*, 2008, 130, 14217.
69. P. Wu, K. Hwang, T. Lan, Y. Lu, *J. Am. Chem. Soc.*, 2013, 135, 5254.
70. J. Liu, Y. Lu, *Angew. Chem. Int. Ed.*, 2006, 45, 90.
71. L. Sutarlie, K. M. Moh, M. G. L. Lim, S. Lukman, E. Cheung, X. Su, *Plasmonics*, 2014, DOI 10.1007/s11468-013-9655-2.
72. R. Levy, N. T. K. Thanh, R. C. Doty, I. Hussain, R. J. Nichols, D. J. Schiffrin, M. Brust, D. G. Fernig, *J. Am. Chem. Soc.*, 2004, 126, 10076.
73. P. Chen, R. Selegard, D. Aili, B. Liedberg, *Nanoscale*, 2013, 5, 8973.
74. X. Liu, Y. Wang, P. Chen, Y. Wang, J. Zhang, D. Aili, B. Liedberg, *Anal. Chem.*, 2014, 86, 2345.
75. P. C. Patel, D. A. Giljohann, D. S. Seferos, C. A. Mirkin, *Proc. Natl. Acad. Sci. U. S. A.*, 2008, 105, 17222.
76. H. S. Mader, P. Kele, S. M. Saleh, O. S. Wolfbeis, *Curr. Opin. Chem. Biol.*, 2010, 14, 582.
77. F. Wang, X. Liu, *Chem. Soc. Rev.*, 2009, 38, 976.
78. J. Zhou, Z. Liu, F. Li, *Chem. Soc. Rev.*, 2012, 41, 1323.
79. L. Sun, Y. Wang, C. Yan, *Acc. Chem. Res.*, 2014, 47, 1001-1009.
80. C. T. Xu, Q. Zhan, H. Liu, G. Somesfalean, J. Qian, S. He, S. Andersson-Engels, *Laser Photonics Rev.*, 2013, 7, 663.
81. L. Wang, Y. Li, *Chem. Mater.*, 2007, 19, 727.
82. F. Wang, X. Liu, *J. Am. Chem. Soc.*, 2008, 130, 5642.
83. K. W. Kramer, D. Biner, G. Frei, H. U. Gudel, M. P. Hehlen, S. R. Muthi, *Chem. Mater.*, 2004, 16, 1244.
84. G. S. Yi, G. M. Chow, *Adv. Funct. Mater.*, 2006, 16, 2324.
85. H.-X. Mai, Y.-W. Zhang, R. Si, Z.-G. Yan, L.-D. Sun, L.-P. You, C.-H. Yan, *J. Am. Chem. Soc.*, 2006, 128, 6426.
86. X. Wang, J. Zhuang, Q. Peng, Y. Li, *Inorg. Chem.* 2006, 45, 6661.
87. Z. Li, Y. Zhang, *Angew. Chem. Int. Ed.*, 2006, 45, 7732.
88. Z. Chen, H. Chen, H. Hu, M. Yu, F. Li, Q. Zhang, Z. Zhou, T. Yi, C. Huang, *J. Am. Chem. Soc.*, 2008, 130, 3023.
89. L.-L. Li, P. Wu, K. Hwang, Y. Lu, *J. Am. Chem. Soc.*, 2013, 135, 2411.
90. F. Wang, D. Banerjee, Y. Liu, X. Chen, X. Liu, *Analyst*, 2010, 135, 1839.
91. K. S. Novoselov, A. K. Geim, S. V. Morozov, D. Jiang, Y. Zhang, S. V. Dubonos, I. V. Grigorieva, A. A. Firsov, *Science*, 2004, 306, 666.
92. M. D. Stoller, S. Park, Y. Zhu, J. An, R. S. Ruoff, *Nano Lett.*, 2008, 8, 3498.
93. C. N. R. Rao, A. K. Sood, K. S. Subrahmanyam, A. Govindaraj, *Angew. Chem. Int. Ed.*, 2009, 48, 7752.
94. H.-H. Lu, C.-L. Zhu, J. Li, J.-J. Liu, X. Chen, H.-H. Yang, *Chem. Commun.*, 2010, 46, 3116.
95. Y. Wang, Z. Li, J. Wang, J. Li, Y. Lin, *Trends Biotechnol.*, 2011, 29, 205.
96. L. Feng, L. Wu, X. Qu, *Adv. Mater.*, 2013, 25, 168.
97. D. Li, R. B. Kaner, *Science*, 2008, 320, 1170.
98. S. Park, R. S. Ruoff, *Nat. Nanotechnol.*, 2009, 4, 127.
99. Q. H. Wang, M. C. Hersam, *Nat. Chem.*, 2009, 1, 40.
100. X. Li, W. Cai, J. An, S. Kim, J. Nah, D. Yang, R. Piner, A. Velamakanni, I. Jung, E. Tutuc, S. K. Banerjee, L. Colombo, R. S. Ruoff, *Science*, 2009, 324, 1312.
101. M. J. Allen, V. C. Tung, R. B. Kaner, *Chem. Rev.*, 2010, 110, 132.
102. M. Choucair, P. Thordarson, J. A. Stride, *Nat. Nanotechnol.*, 2009, 4, 30.
103. X. Fan, W. Peng, Y. Li, X. Li, S. Wang, G. Zhang, F. Zhang, *Adv. Mater.*, 2008, 20, 4490.

104. D. Tasis, N. Tagmatarchis, A. Bianco, M. Prato, *Chem. Rev.*, 2006, 106, 1105.
105. W. Yang, K. R. Ratinac, S. P. Ringer, P. Thordarson, J. J. Gooding, F. Braet, *Angew. Chem. Int. Ed.*, 2010, 49, 2114.
106. S. Lijima, *Nature*, 1991, 354, 56.
107. L. Lacerda, S. Raffà, M. Prato, A. Bianco, K. Kostarelos, *NanoToday*, 2007, 2, 38.
108. S. He, B. Song, D. Li, C. Zhu, W. Qi, Y. Wen, L. Wang, S. Song, H. Fang, C. Fan, *Adv. Funct. Mater.*, 2010, 20, 453.
109. R. Yang, Z. Tang, J. Yan, H. Kang, Y. Kim, Z. Zhu, W. Tan, *Anal. Chem.*, 2008, 80, 7408.
110. B. C. Satishkumar, L. O. Brown, Y. Gao, C.-C. Wang, H.-L. Wang, S. K. Doorn, *Nat. Nanotechnol.*, 2007, 2, 560.
111. D. Cui, B. Pan, H. Zhang, F. Gao, R. Wu, J. Wang, R. He, T. Asahi, *Anal. Chem.*, 2008, 80, 7996.
112. D. A. Heller, H. Jin, B. M. Martinez, D. Patel, B. M. Miller, T.-K. Yeung, P. V. Jena, C. Hobartner, T. Ha, S. K. Silverman, M. S. Strano, *Nat. Nanotechnol.*, 2009, 4, 114.
113. H. Li, Z. Kang, Y. Liu, S.-T. Lee, *J. Mater. Chem.*, 2012, 22, 24230.
114. X. Xu, R. Ray, Y. Gu, H. J. Ploehn, L. Gearheart, K. Raker, W. A. Scrivens, *J. Am. Chem. Soc.*, 2004, 126, 12736.
115. S. N. Baker, G. A. Baker, *Angew. Chem. Int. Ed.*, 2010, 49, 6726.
116. X. Hu, L. Cheng, N. Wang, L. Sun, W. Wang, W. Liu, *RSC Adv.*, 2014, 4, 18818.
117. S.-L. Hu, K.-Y. Niu, J. Sun, J. Yang, N.-Q. Zhao, X.-W. Du, *J. Mater. Chem.*, 2009, 19, 484.
118. J. Zhou, C. Booker, R. Li, X. Zhou, T.-K. Sham, X. Sun, Z. Ding, *J. Am. Chem. Soc.*, 2007, 129, 744.
119. Y.-P. Sun, X. Wang, F. Lu, L. Cao, M. J. Meziani, P. G. Luo, L. Gu, L. M. Veca, *J. Phys. Chem. C*, 2008, 112, 18295.
120. H. Zhu, X. Wang, Y. Li, Z. Wang, F. Yang, X. Yang, *Chem. Commun.*, 2009, 5118.
121. H. Peng, J. Travas-Sejdic, *Chem. Mater.*, 2009, 21, 5563.
122. L. Tian, D. Ghosh, W. Chen, S. Pradhan, X. Chang, S. Chen, *Chem. Mater.*, 2009, 21, 2803.
123. A. B. Bourlinos, A. Stassinopoulos, D. Anglos, R. Zboril, M. Karakassides, E. P. Giannelis, *small*, 2008, 4, 455.
124. A. B. Bourlinos, A. Stassinopoulos, D. Anglos, R. Zboril, V. Georgakilas, E. P. Giannelis, *Chem. Mater.*, 2008, 20, 4539.
125. H. Liu, T. Ye, C. Mao, *Angew. Chem. Int. Ed.*, 2007, 46, 6473.
126. Q.-L. Zhao, Z.-L. Zhang, B.-H. Huang, J. Peng, M. Zhang, D.-W. Pang, *Chem. Commun.*, 2008, 5116.
127. Y.-P. Sun, B. Zhou, Y. Lin, W. Wang, K. A. S. Fernando, P. Pathak, M. J. Meziani, B. A. Harruff, X. Wang, H. Wang, P. G. Luo, H. Yang, M. E. Kose, B. Chen, L. M. Veca, S.-Y. Xie, *J. Am. Chem. Soc.*, 2006, 128, 7756.
128. X. Wang, L. Cao, F. Lu, M. J. Meziani, H. Li, G. Qi, B. Zhou, B. A. Harruff, F. Kermarrec, Y.-P. Sun, *Chem. Commun.*, 2009, 3774.
129. S. C. Ray, A. Saha, N. R. Jana, R. Sarker, *J. Phys. Chem. C*, 2009, 113, 18546.
130. S.-T. Yang, L. Cao, P. G. Luo, F. Lu, X. Wang, H. Wang, M. J. Meziani, Y. Liu, G. Qi, Y.-P. Sun, *J. Am. Chem. Soc.*, 2009, 131, 11308.
131. S.-T. Yang, X. Wang, H. Wang, F. Lu, P. G. Luo, L. Cao, M. J. Meziani, J.-H. Liu, M. Chen, Y. Huang, Y.-P. Sun, *J. Phys. Chem. C*, 2009, 113, 18110.
132. L. Cao, X. Wang, M. J. Meziani, F. Lu, H. Wang, P. G. Luo, Y. Lin, B. A. Harruff, L. M. Veca, D. Murray, S.-Y. Xie, Y.-P. Sun, *J. Am. Chem. Soc.*, 2007, 129, 11318.
133. H. X. Zhao, L. Q. Liu, Z. D. Liu, Y. Wang, X. J. Zhao, C. Z. Huang, *Chem. Commun.*, 2011, 47, 2604.
134. W. Wei, C. Xu, J. Ren, B. Xu, X. Qu, *Chem. Commun.*, 2012, 48, 1284.
135. W. Shi, Q. Wang, Y. Long, Z. Cheng, S. Chen, H. Zheng, Y. Huang, *Chem. Commun.*, 2011, 47, 6695.
136. T. Förster, *Ann. Phys.*, 1948, 6, 55.
137. T. Rantanen, M.-L. Jarvenpää, J. Vuojola, K. Kuningas, T. Soukka, *Angew. Chem. Int. Ed.*, 2008, 47, 3811.
138. X. M. Hua, J. I. Gersten, A. Nitzan, *J. Chem. Phys.*, 1985, 83, 3650.
139. J. Zhang, Y. Fu, J. R. Lakowicz, *J. Phys. Chem. C*, 2007, 111, 50.
140. J. Zhang, Y. Fu, M. H. Chowdhury, J. R. Lakowicz, *J. Phys. Chem. C*, 2007, 111, 11784.
141. T. Förster, *Discuss. Faraday Soc.*, 1959, 27, 7.
142. K. E. Sapsford, L. Berti, I. L. Medintz, *Angew. Chem. Int. Ed.*, 2006, 45, 4562.
143. T. Sen, K. K. Haldar, A. Patra, *J. Phys. Chem. C*, 2008, 112, 17945.
144. C. S. Yun, A. Javier, T. Jennings, M. Fisher, S. Hira, S. Peterson, B. Hopkins, N. O. Reich, G. F. Strouse, *J. Am. Chem. Soc.*, 2005, 127, 3115.
145. T. L. Jennings, M. P. Singh, G. F. Strouse, *J. Am. Chem. Soc.*, 2006, 128, 5462.
146. P. C. Ray, A. Fortner, G. K. Darbha, *J. Phys. Chem. B*, 2006, 110, 20745.
147. L. Feng, H. Li, Y. Qu, C. Lv, *Chem. Commun.*, 2012, 48, 4633.
148. W. R. A. U. J. Krull, *Anal. Bioanal. Chem.*, 2008, 391, 1609.
149. S. Mayilo, M. A. Kloster, M. Wunderlich, A. Lutich, T. A. Klar, A. Nichtl, K. Kurzinger, F. D. Stefani, J. Feldmann, *Nano Lett.*, 2009, 9, 4558.
150. S. Y. Lim, J. H. Kim, J. S. Lee, C. B. Park, *Langmuir*, 2009, 25, 13302.
151. N. Zhang, Y. Liu, L. Tong, K. Xu, L. Zhuo, B. Tang, *Analyst*, 2008, 133, 1176.
152. B. Tang, L. Cao, K. Xu, L. Zhuo, J. Ge, Q. Li, L. Yu, *Chem. Eur. J.*, 2008, 14, 3637.
153. C. Zhang, Y. Yuan, S. Zhang, Y. Wang, Z. Liu, *Angew. Chem. Int. Ed.*, 2011, 50, 6851.
154. X. Wang, X. Guo, *Analyst*, 2009, 134, 1348.
155. J. Liu, J. H. Lee, Y. Lu, *Anal. Chem.*, 2007, 79, 4120.
156. C.-C. Huang, H.-T. Chang, *Anal. Chem.*, 2006, 78, 8332.
157. G. K. Darbha, A. Ray, P. C. Ray, *ACS Nano*, 2007, 1, 208.
158. L. Zhou, Y. Lin, Z. Huang, J. Ren, X. Qu, *Chem. Commun.*, 2012, 48, 1147.
159. L. Li, F. Gao, J. Ye, Z. Chen, Q. Li, W. Gao, L. Ji, R. Zhang, B. Tang, *Anal. Chem.*, 2013, 85, 9721.
160. M. Xue, X. Wang, L. Duan, W. Gao, L. Ji, B. Tang, *Biosens. Bioelectron.*, 2012, 36, 168.
161. Y. Wen, F. Xing, S. He, S. Song, L. Wang, Y. Long, D. Li, C. Fan, *Chem. Commun.*, 2010, 46, 2596.
162. H. Wang, Y. Wang, J. Jin, R. Yang, *Anal. Chem.*, 2008, 80, 9021.
163. C. Liu, Z. Wang, H. Jia, Z. Li, *Chem. Commun.*, 2011, 47, 4661.
164. D. Zheng, D. S. Seferos, D. A. Giljohann, P. C. Patel, C. A. Mirkin, *Nano Lett.*, 2009, 9, 3258.
165. Y. Wang, Z. Li, D. Hu, C.-T. Lin, J. Li, Y. Lin, *J. Am. Chem. Soc.*, 2010, 132, 9274.
166. Y. Shi, W. T. Huang, H. Q. Luo, N. B. Li, *Chem. Commun.*, 2011, 47, 4676.
167. S. Wu, N. Duan, X. Ma, Y. Xia, H. Wang, Z. Wang, Q. Zhang, *Anal. Chem.*, 2012, 84, 6263.
168. B. Tang, N. Zhang, Z. Chen, K. Xu, L. Zhuo, L. An, G. Yang, *Chem. Eur. J.*, 2008, 14, 522.
169. M. Liu, Q. Zhang, H. Zhao, S. Chen, H. Yu, Y. Zhang, X. Quan, *Chem. Commun.*, 2011, 47, 4084.
170. F. Li, Y. Feng, C. Zhao, P. Li, B. Tang, *Chem. Commun.*, 2012, 48, 127.
171. X.-H. Zhao, R.-M. Kong, X.-B. Zhang, H.-M. Meng, W.-N. Liu, W. Tan, G.-L. Shen, R.-Q. Yu, *Anal. Chem.*, 2011, 83, 5062.
172. J. Zhang, L. Wang, H. Zhang, F. Boey, S. Song, C. Fan, *small*, 2010, 6, 201.
173. C.-Y. Zhang, H.-C. Yeh, M. T. Kuroki, T.-H. Wang, *Nat. Mater.*, 2005, 4, 826.

174. P. Zhang, S. Rogelj, K. Nguyen, D. Wheeler, *J. Am. Chem. Soc.*, 2006, 128, 12410.
175. Z. Dai, J. Zhang, Q. Dong, N. Guo, S. Xu, B. Sun, Y. Bu, *Chin. J. Chem. Eng.*, 2007, 15, 791.
176. C.-H. Lu, H.-H. Yang, C.-L. Zhu, X. Chen, G.-N. Chen, *Angew. Chem. Int. Ed.*, 2009, 48, 4785.
177. C.-H. Lu, J. Li, J.-J. Liu, H.-H. Yang, X. Chen, G.-N. Chen, *Chem. Eur. J.*, 2010, 16, 4889.
178. H. Dong, W. Gao, F. Yan, H. Ji, H. Ju, *Anal. Chem.*, 2010, 82, 5511.
179. F. Li, Y. Huang, Q. Yang, Z. Zhong, D. Li, L. Wang, S. Song, C. Fan, *Nanoscale*, 2010, 2, 1021.
180. R. Yang, J. Jin, Y. Chen, N. Shao, H. Kang, Z. Xiao, Z. Tang, Y. Wu, Z. Zhu, W. Tan, *J. Am. Chem. Soc.*, 2008, 130, 8351.
181. B. Dubertret, M. Calame, A. J. Libchaber, *Nat. Biotechnol.*, 2001, 19, 365.
182. S. Song, Z. Liang, J. Zhang, L. Wang, G. Li, C. Fan, *Angew. Chem. Int. Ed.*, 2009, 48, 8670.
183. D. J. Maxwell, J. R. Taylor, S. Nie, *J. Am. Chem. Soc.*, 2002, 124, 9606.
184. K. Wang, Z. Tang, C. J. Yang, Y. Kim, X. Fang, W. Li, Y. Wu, C. D. Medley, Z. Cao, J. Li, P. Colon, H. Lin, W. Tan, *Angew. Chem. Int. Ed.*, 2008, 48, 856.
185. N. E. Broude, *Trends Biotechnol.*, 2002, 20, 249.
186. S. Tyagi, D. P. Bratu, F. R. Kramer, *Nat. Biotechnol.*, 1998, 16, 49-53.
187. S. Tyagi, F. R. Kramer, *Nat. Nanotechnol.*, 1996, 14, 303.
188. H. Li, M. Wang, C. Wang, W. Li, W. Qiang, D. Xu, *Anal. Chem.*, 2013, 85, 4492.
189. S. Nie, S. R. Emory, *Science*, 1997, 275, 1102.
190. E. S. Jeng, A. E. Moll, A. C. Roy, J. B. Gastala, M. S. Strano, *Nano Lett.*, 2006, 6, 371.
191. E. Oh, M.-Y. Hong, D. Lee, S.-H. Nam, H. C. Yoon, H.-S. Kim, *J. Am. Chem. Soc.*, 2005, 127, 3270.
192. H. Chang, L. Tang, Y. Wang, J. Jiang, J. Li, *Anal. Chem.*, 2010, 82, 2341.
193. Y.-M. Wu, Y. Cen, L.-J. Huang, R.-Q. Yu, X. Chu, *Chem. Commun.*, 2014, 50, 4759.
194. X. Wang, C. Wang, K. Qu, Y. Song, J. Ren, D. Miyoshi, N. Sugimoto, X. Qu, *Adv. Funct. Mater.*, 2010, 20, 3967.
195. S. Lukman, K. M. M. Aung, J. Liu, B. Liu, X. Su, *ACS Appl. Mater. Interfaces*, 2013, 5, 12725.
196. S. Lukman, K. M. M. Aung, M. G. L. Lim, S. Hong, S. K. Tan, E. Cheung, X. Su, *RSC Adv.*, 2014, 4, 8883.
197. S. Lee, E.-J. Cha, K. Park, S.-Y. Lee, J.-K. Hong, I.-C. Sun, S. Y. Kim, K. Choi, I. C. Kwon, K. Kim, C.-H. Ahn, *Angew. Chem. Int. Ed.*, 2008, 2804.
198. J. Li, C.-H. Lu, Q.-H. Yao, X.-L. Zhang, J.-J. Liu, H.-H. Yang, G.-N. Chen, *Biosens. Bioelectron.*, 2011, 26, 3894.
199. H. Wang, Q. Zhang, X. Chu, T. Chen, J. Ge, R. Yu, *Angew. Chem. Int. Ed.*, 2011, 50, 7065.
200. K. Boeneman, B. C. Mei, A. M. Dennis, G. Bao, J. R. Deschamps, H. mattoussi, I. L. Medintz, *J. Am. Chem. Soc.*, 2009, 131, 3828.
201. H. Yao, Y. Zhang, F. Xia, Z. Xia, J. Rao, *Angew. Chem. Int. Ed.*, 2007, 46, 4346.
202. I. L. Medintz, A. R. Clapp, F. M. Brunel, T. Tiefenbrunn, H. T. Uyeda, E. L. Chang, J. R. Deschamps, P. E. Dawson, H. Mattoussi, *Nat. Mater.*, 2006, 5, 581.
203. J. C. Breger, K. E. Sapsford, J. Ganek, K. Susumu, M. H. Stewart, I. L. Medintz, *ACS Appl. Mater. Interfaces*, 2014, 6, 11529.
204. D. Feng, Y. Zhang, T. Feng, W. Shi, X. Li, H. Ma, *Chem. Commun.*, 2011, 47, 10680.
205. L. Wang, R. Yan, Z. Huo, L. Wang, J. Zeng, J. Bao, X. Wang, Q. Peng, Y. Li, *Angew. Chem. Int. Ed.*, 2005, 44, 6054.
206. M. Wang, W. Hou, C. Mi, W. Wang, Z. Xu, H. Teng, C. Mao, S. Xu, *Anal. Chem.*, 2009, 81, 8783.
207. K. J. Oh, K. J. Cash, V. Hugenberg, K. W. Plaxco, *Bioconjugate Chem.*, 2007, 18, 607.
208. K. J. Oh, K. J. Cash, K. W. Plaxco, *Chem. Eur. J.*, 2009, 15, 2244.
209. K. J. Oh, K. J. Cash, K. W. Plaxco, *J. Am. Chem. Soc.*, 2006, 128, 14018.
210. S. Thurlley, L. Roglin, O. Seitz, *J. Am. Chem. Soc.*, 2007, 129, 12693.
211. M. Suzuki, Y. Husimi, H. Komatsu, K. Suzuki, K. T. Douglas, *J. Am. Chem. Soc.*, 2008, 130, 5720.
212. G. Liu, J. Wang, D. S. Wunschel, Y. Lin, *J. Am. Chem. Soc.*, 2006, 128, 12382.
213. Y. Wang, D. V. Zagorevski, M. R. Lennartz, D. J. Loegering, J. A. Steken, *Anal. Chem.*, 2009, 81, 9961.
214. H. Jang, Y.-K. Kim, H.-M. Kwon, W.-S. Yeo, D.-E. Kim, D.-H. Min, *Angew. Chem. Int. Ed.*, 2010, 49, 5703.
215. J. E. Ghadiali, S. B. Lowe, M. M. Stevens, *Angew. Chem.*, 2011, 123, 3479.
216. W. Wu, H. Hu, F. Li, L. Wang, J. Gao, J. Lu, C. Fan, *Chem. Commun.*, 2011, 47, 1201.
217. W. R. Algar, M. G. Ancona, A. P. Malanoski, K. Susumu, I. L. Medintz, *ACS Nano*, 2012, 6, 11044.
218. P. Biswas, L. N. Cella, S. H. Kang, A. Mulchandani, M. V. yates, W. Chen, *Chem. Commun.*, 2011, 47, 5259.
219. J. H. Kim, B. H. Chung, *small*, 2010, 6, 126.
220. D. M. Jameson, J. A. Ross, *Chem. Rev.*, 2010, 110, 2685.
221. X. Fang, Z. Cao, T. Beck, W. Tan, *Anal. Chem.*, 2001, 73, 5752.
222. G. Gokulrangan, J. R. Unruh, D. F. Holub, B. Ingram, C. K. Johnson, G. S. Wilson, *Anal. Chem.*, 2005, 77, 1963.
223. D. Zhang, Q. Zhao, B. Zhao, H. Wang, *Anal. Chem.*, 2012, 84, 3070.
224. W. Li, K. Wang, W. Tan, C. Ma, X. Yang, *Analyst*, 2007, 132, 107.
225. M. Zou, Y. Chen, X. Xu, H. Huang, F. Liu, N. Li, *Biosens. Bioelectron.*, 2012, 32, 148.
226. L. Cui, Y. Zou, N. Lin, Z. Zhu, G. Jenkins, C. J. Yang, *Anal. Chem.*, 2012, 84, 5535.
227. Z. Zhu, C. Ravelet, S. Perrier, V. Guieu, E. Fiore, E. Peyrin, *Anal. Chem.*, 2012, 84, 7203.
228. Y. Qiao, H. Tang, G. R. Munske, P. Dutta, C. F. Ivory, W.-J. Dong, *J. Fluoresc.*, 2011, 21, 2101.
229. B.-C. Ye, B.-C. Yin, *Angew. Chem. Int. Ed.*, 2008, 47, 8386.
230. Y. Huang, S. Zhao, Z.-F. Chen, Y.-C. Liu, H. Liang, *Chem. Commun.*, 2011, 47, 4763.
231. Y. Yu, Y. Liu, S. J. Zhen, C. Z. Huang, *Chem. Commun.*, 2013, 49, 1942.
232. J. Liu, C. Wang, Y. Jiang, Y. Hu, J. Li, S. Yang, Y. Li, R. Yang, W. Tan, C. Z. Huang, *Anal. Chem.*, 2013, 85, 1424.
233. Y. Huang, S. Zhao, Z.-F. Chen, M. Shi, H. Liang, *Chem. Commun.*, 2012, 48, 7480.
234. Y. Huang, J. Chen, M. Shi, S. Zhao, Z.-F. Chen, H. Liang, *J. Mater. Chem. B*, 2013, 1, 2018.
235. J.-M. Nam, C. S. Thaxton, C. A. Mirkin, *Science*, 2003, 301, 1884.
236. C. S. Thaxton, D. G. Georganopoulou, C. A. Mirkin, *Clinica Chimica Acta*, 2006, 363, 120.
237. S. Brakmann, *Angew. Chem. Int. Ed.*, 2004, 43, 5730.
238. T. A. Taton, C. A. Mirkin, R. L. Letsinger, *Science*, 2000, 289, 1757.
239. C. S. Thaxton, R. Elghanian, A. D. Thomas, S. I. Stoeva, J.-S. Lee, N. D. Smith, A. J. Schaeffer, H. Klocker, W. Horninger, G. Bartsch, C. A. Mirkin, *Proc. Natl. Acad. Sci. U.S.A.*, 2009, 106, 18437.
240. D. G. Georganopoulou, L. Chang, J.-M. Nam, C. S. Thaxton, E. J. Mufson, W. L. Klein, C. A. Mirkin, *Proc. Natl. Acad. Sci. U. S. A.*, 2005, 102, 2273.
241. E.-Y. Kim, J. Stanton, B. T. Korber, K. Krebs, D. Bogdan, K. Kunstman, S. Wu, J. P. Phair, C. A. Mirkin, S. M. Wolinsky, *Nanomedicine*, 2008, 3, 293.

- 1
2
3
4
5
6
7
8
9
10
11
12
13
14
15
16
17
18
19
20
21
22
23
24
25
26
27
28
29
30
31
32
33
34
35
36
37
38
39
40
41
42
43
44
45
46
47
48
49
50
51
52
53
54
55
56
57
58
59
60
242. H.-q. Yin, M.-x. Jia, L.-j. Shi, S. Yang, L.-y. Zhang, Q.-m. Zhang, S.-q. Wang, G. Li, J.-g. Zhang, *J. Virol. Methods*, 2011, 178, 225.
243. E. D. Goluch, J.-M. Nam, D. G. Georganopoulou, T. N. Chiesl, K. A. Shaikh, K. S. Ryu, A. E. Barron, C. A. Mirkin, C. Liu, *Lab Chip*, 2006, 6, 1293.
244. J.-M. Nam, S. I. Stoeva, C. A. Mirkin, *J. Am. Chem. Soc.*, 2004, 126, 5932.
245. C. S. Thaxton, H. D. Hill, D. G. Georganopoulou, S. I. Stoeva, C. A. Mirkin, *Anal. Chem.*, 2005, 77, 8174.
246. H. D. Hill, C. A. Mirkin, *Nat. Protoc.*, 2006, 1, 324.
247. Y. P. Bao, T.-F. Wei, P. A. Lafebvre, H. An, L. He, G. T. Kunkel, U. R. Muller, *Anal. Chem.*, 2006, 78, 2055.
248. J.-M. Nam, A. R. Wise, J. T. Groves, *Anal. Chem.*, 2005, 77, 6985.
249. J.-M. Nam, K.-J. Jang, J. T. Groves, *Nat. Protoc.*, 2007, 2, 1438.
250. B.-K. Oh, J.-M. Nam, S. W. Lee, C. A. Mirkin, *small*, 2006, 2, 103.
251. D. Zhu, Y. Tang, D. Xing, W. R. Chen, *Anal. Chem.*, 2008, 80, 3566.
252. C. Cao, R. Dhumpa, D. D. Bang, Z. Ghavifekr, J. Hogberg, A. Wolff, *Analyst*, 2010, 135, 337.
253. D. Zhang, D. J. Carr, E. C. Alocilja, *Biosens. Bioelectron.*, 2009, 24, 1377.
254. M. Trevisan, M. Schawaller, G. Quapil, E. Souteyrand, Y. Merieux, J.-P. Cloarec, *Biosens. Bioelectron.*, 2010, 26, 1631.
255. P. He, L. Shen, Y. Cao, D. Li, *Anal. Chem.*, 2007, 79, 8024.
256. X. Zhang, H. Su, S. Bi, S. Li, S. Zhang, *Biosens. Bioelectron.*, 2009, 24, 2730.
257. X. Zhang, B. Qi, Y. Li, S. Zhang, *Biosens. Bioelectron.*, 2009, 25, 259.
258. Y. Li, B. Liu, X. Li, Q. Wei, *Biosens. Bioelectron.*, 2010, 25, 2543.
259. D. Zhang, M. C. Huarng, E. C. Alocilja, *Biosens. Bioelectron.*, 2010, 26, 1736.
260. L. Shen, Z. Chen, Y. Li, S. He, S. Xie, X. Xu, Z. Liang, X. Meng, Q. Li, Z. Zhu, M. Li, M. Li, X. C. Le, Y. Shao, *Anal. Chem.*, 2008, 80, 6323.
261. H. D. Hill, R. A. Vega, C. A. Mirkin, *Anal. Chem.*, 2007, 79, 9218.
262. S. I. Stoeva, J.-S. Lee, J. E. Smith, S. T. Rosen, C. A. Mirkin, *J. Am. Chem. Soc.*, 2006, 128, 8378.
263. M. He, K. Li, J. Xiao, Y. Zhou, *J. Virol. Methods*, 2008, 151, 126.
264. J. Li, S. Song, X. Liu, L. Wang, D. Pan, Q. Huang, Y. Zhao, C. Fan, *Adv. Mater.*, 2008, 20, 497.
265. S. Bi, Y. Yan, X. Yang, S. Zhang, *Chem. Eur. J.*, 2009, 15, 4704.
266. Y. Huang, S. Zhao, Z.-F. Chen, M. Shi, J. Chen, H. Liang, *Chem. Commun.*, 2012, 48, 11877.
267. J. Li, S. Song, D. Li, Y. Su, Q. Huang, Y. Zhao, C. Fan, *Biosens. Bioelectron.*, 2009, 24, 3311.
268. F. Qu, T. Li, M. Yang, *Biosens. Bioelectron.*, 2011, 26, 3927.
269. Y. Song, K. Qu, C. Xu, J. Ren, X. Qu, *Chem. Comm.*, 2010, 46, 6572.
270. M. Liu, H. Zhao, S. Chen, H. Yu, X. Quan, *ACS Nano*, 2012, 6, 3142.
271. Y. Guo, L. Deng, J. Li, S. Guo, E. Wang, S. Dong, *ACS Nano*, 2011, 5, 1282.
272. H. F. Krug, P. Wick, *Angew. Chem. Int. Ed.*, 2011, 50, 1260.
273. N. Lewinski, V. Colvin, R. Drezek, *small*, 2008, 4, 26.
274. S. A. Minaker, K. D. Daze, M. C. F. Ma, F. Hof, *J. Am. Chem. Soc.*, 2012, 134, 11674.
275. S. S. Chou, M. De, J. Luo, V. M. Rotello, J. Huang, V. P. Dravid, *J. Am. Chem. Soc.*, 2012, 134, 16725.

ARTICLE

Table 1 Nanomaterials used for constructing dual-transducer biosensors

Nanomaterial	Favorable Properties	Major Roles in Design	Challenges	Other Remarks
QDs	<ul style="list-style-type: none"> Tunable fluorescence (Figure 1) Photostability Emission brightness 	<ul style="list-style-type: none"> FRET donor (More Preferential) FRET acceptor 	<ul style="list-style-type: none"> Cytotoxicity⁴³ Fluorescence blinking No standard synthetic protocol 	<ul style="list-style-type: none"> Surface functionalization required to increase aqueous solubility and biocompatibility
Metal NP	<ul style="list-style-type: none"> LSPR absorption (Figure 2) Light scattering Facile surface modification (e.g. Au-thiol interaction) Intrinsic affinity to ssDNA and proteins through coordination chemistry 	<ul style="list-style-type: none"> Fluorescence quencher/enhancer Fluorescence polarization amplifier Carrier for DNA barcode or CL reaction catalyzers 	<ul style="list-style-type: none"> Non-specific aggregation (e.g. during particle surface modification or assaying procedures) 	<ul style="list-style-type: none"> Size-dependent optical behavior (e.g., Absorption dominates for AuNPs <80nm; Scattering for any larger ones)⁷¹ Various other particle shapes (e.g. rods, plates, triangles, stars.) to provide tunable absorption spectra
UCNPs	<ul style="list-style-type: none"> NIR excitation (Figure 3) Photostability 	<ul style="list-style-type: none"> FRET donor 	<ul style="list-style-type: none"> Low quantum yield⁷⁷ NIR heating effect⁸⁰ 	<ul style="list-style-type: none"> Reduced background noises relative to organic dyes and QDs⁹⁰ Surface modification required to increase aqueous solubility and biocompatibility
Graphene, GO, CNT	<ul style="list-style-type: none"> Optical quenching (Figure 4) Different binding affinity with ds- and ssDNA Enzyme mimicking 	<ul style="list-style-type: none"> Fluorescence quencher Fluorescence polarization amplifier CL reaction catalyzer 	<ul style="list-style-type: none"> Non-specific adsorption CNT structure heterogeneity 	<ul style="list-style-type: none"> GO is more commonly used than intact graphene. Intrinsically suitable for multiplexed sensing because of large surface area
Carbon Nanodot	<ul style="list-style-type: none"> Tunable fluorescence Facile synthesis Low fabrication cost 	<ul style="list-style-type: none"> FRET donor 	<ul style="list-style-type: none"> Lack of thorough understanding on physical and chemical properties 	<ul style="list-style-type: none"> Usually need further surface modification (e.g. ligand attachment or solid capping layers) for efficient emission^{115, 117}

Table 2 Selected examples of the FRET assays for metal ions and small molecules detection

Assay Type	Target	Donor	Acceptor	Sensing Probe	LOD	Reference
	Cholesterol	Fluorescein	AuNP	β -cyclodextrin	9 nM	Ref. 151
	Glucose	CdTe QDs	AuNP	Concanavalin A	50 nM	Ref. 152
	Glucose	UCNPs	GO	ConA and Chitosan	25 nM	Ref. 153
	K ⁺	CDs	rGO	18-crown-6 ether	10 μ M	Ref. 134
	Pb ²⁺	CdTe QDs	AuNP	11-mercaptopundecanoic acid	30 ppb (~146 nM)	Ref. 154
Figure 6 Scheme A [Competition]	Adenosine; Cocaine	QDs	AuNP	Adenosine Aptamer; Cocaine Aptamer	50 μ M; 120 μ M	Ref. 155
	Hg ²⁺	Rhodamine B	AuNP	Nil	10 pM	Ref. 156
	Hg ²⁺	CDs	Hg ²⁺	Nil	4.2 nM	Ref. 157
	Biothiols	CDs	Hg ²⁺	Nil	4.9–8.5 nM	Ref. 158
	Glucose	FITC	AuNP	dextran	5 nM	Ref. 159
	F ⁻	CdTe QDs	AuNP	Boronate Ester	50 nM	Ref. 160
	Ag ⁺	FAM	GO	C-rich ssDNA	5 nM	Ref. 161
	Hg ²⁺	FAM	GO	T-rich ssDNA	30 nM	Ref. 108
	Hg ²⁺	UCNP	GO	T-rich ssDNA	0.5 nM	Ref. 162
Figure 6 Scheme B [Competition]	ATP	Cy5	AuNP	Aptamer	mM level	Ref. 163
	ATP	FAM	GO	Aptamer	μ M level	Ref. 164
	Adenosine	FAM	GO	Aptamer	10 μ M	Ref. 165
	ATP	UCNPs	GO	Aptamer	80 nM	Ref. 108
	Hemin	Acridine Orange	GO	Aptamer	50 nM	Ref. 163
	Mycotoxins	UCNPs	GO	Aptamer	fM level	Ref. 166
Figure 6 Scheme C [Cleavage]	•OH	FAM	AuNP	ssDNA	2.4 nM	Ref. 167
	Uranyl	Cy3	AuNP and BHQ-2	DNAzyme Substrate	μ M level	Ref. 168
Figure 6 Scheme D [Cleavage]	•OH	FAM	GO	ssDNA	N.A.	Ref. 69
	BLM	FAM	GO	ssDNA	0.2 nM	Ref. 169
	Pb ²⁺	FAM	GO	DNAzyme Substrate	300 pM	Ref. 170

Table 3 Selected examples of the FRET assays for DNA detection

Assay Type	Target DNA Length	Donor	Acceptor	LOD	Reference
	30 bp	CdSe-ZnS QDs	Cy5	4.8 fM	Ref. 173
	26 bp	UCNP	TAMRA	1.3 nM	Ref. 174
Figure 8					
Scheme A	20 bp	CdSe QDs	MWNT	0.2 pM	Ref. 111
<i>[Crosslinking]</i>					
Figure 8	24 bp	CdTe QDs	AuNP	N.A.	Ref. 175
Scheme B					
<i>[Competition]</i>					
	23 bp	FAM	SWNT	~5 nM	Ref. 109
	17 bp	FAM	GO	100 pM	Ref. 108
Figure 8					
Scheme C	23 bp	FAM	GO	~10 nM	Ref. 176
<i>[Competition]</i>					
	15 bp	FAM or Cy5	GO	2.0 nM	Ref. 177
	22 bp	CdTe QDs	GO	12 nM	Ref. 178
Figure 8	15 bp	FAM	GO (and TAMRA)	0.1 nM	Ref. 179
Scheme D	19 bp	FAM	SWNT	4 nM	Ref. 180
<i>[Competition]</i>					
	16 bp	Rhodamine 6G	AuNP	nM level	Ref. 181
Figure 8					
Scheme E	15 bp	Organic dye	AuNP	nM level	Ref. 182
<i>[Alternation]</i>					
	24 bp	Fluorescein	AuNP	40 nM	Ref. 183

1 Figure 8

2
3 Scheme F

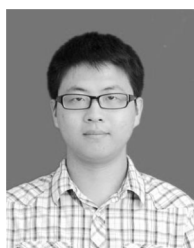
4
5 *[Alternation]*

Table 4 Selected examples of the FRET assays for protein and enzyme detection

Assay Type	Target	Donor	Acceptor	Sensing Probe	LOD	Reference
	Avidin	QDs	AuNP	Biotin	10 nM	Ref. 191
Figure 9 Scheme A [Competition]	Avidin	SWNT	Organic dyes	Biotin	1 nM	Ref. 110
	Thrombin	FAM	GO	Aptamer	31.3 pM	Ref. 192
	Thrombin	FAM	GO	Aptamer	2.0 nM	Ref. 176
Figure 9 Scheme B1 [Competition]	HIV Antibody	UCNP	GO	Polypeptide	2.0 nM	Ref. 193
	Cyclin A2	FITC	GO	Polypeptide	0.5 nM	Ref. 194
	ER α , ER β	CPEs	AuNP	ER binding site (DNA)	N.A.	Ref. 195
Figure 9 Scheme B2 [Competition]	FoxA1, AP-2 γ	CPEs	AuNP	Protein binding site (DNA)	N.A.	Ref. 196
	ER α , ER β	CPEs	AuNP	ER binding site	N.A.	Ref. 195
Figure 9 Scheme C [Linking]	FoxA1, AP-2 γ	CPEs	AuNP	Protein binding site (DNA)	N.A.	Ref. 196
	MMP	Cy5.5	AuNP	Polypeptide	1.0 nM	Ref. 197
	MMP-2	CdSe-ZnS QDs	GO	Polypeptide	nM level	Ref. 198
	S1 Nucleases	Cy3	AuNP	ssDNA	N.A.	Ref. 146
Figure 9 Scheme D [Cleavage]	Caspase-3	FAM	GO	Polypeptide	0.4 nM	Ref. 199
	Caspase-3	QDs	mCherry Fluorescent Protein	Peptide	20 pM	Ref. 200
	MMP-2	Bioluminescent Protein	QD	Peptide	19 ng/mL	Ref. 201

Protease (Caspase 1, Collagenase, chymotrypsin, thrombin)	CdSe-ZnS QDs	Cy3	Peptide	N.A.	Ref. 202
Kallikrein	CdSe/ZnS QDs	Cy3- maleimide	Peptide	N.A.	Ref. 203

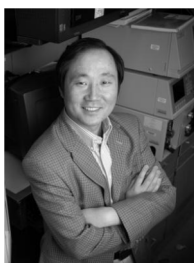
Figure 9	MMP-2	FITC	GO	Polypeptide	50 pM	Ref. 204
Scheme E						
<i>[Cleavage]</i>						



Ning Li obtained his B. Eng from National University of Singapore in 2013. He is an A*STAR scholar and performed his one-year research attachment in Institute of Materials Research and Engineering (IMRE), A*STAR, supervised by Dr. Xiaodi Su. His current research interests focus on the designing of nanomaterial-based biosensors and disease diagnosis techniques.



Dr. Xiaodi Su received her PhD in 1995 from Nankai University, China, majored in Analytical Chemistry. Currently she is a senior scientist in the Institute of Materials Research & Engineering (IMRE), A*STAR, Singapore, heading the Materials Analysis and Characterization capability group. Her research interests include developing advanced analytical technologies for biomedical research and developing biosensors for disease diagnosis, environmental monitoring, and food analysis.

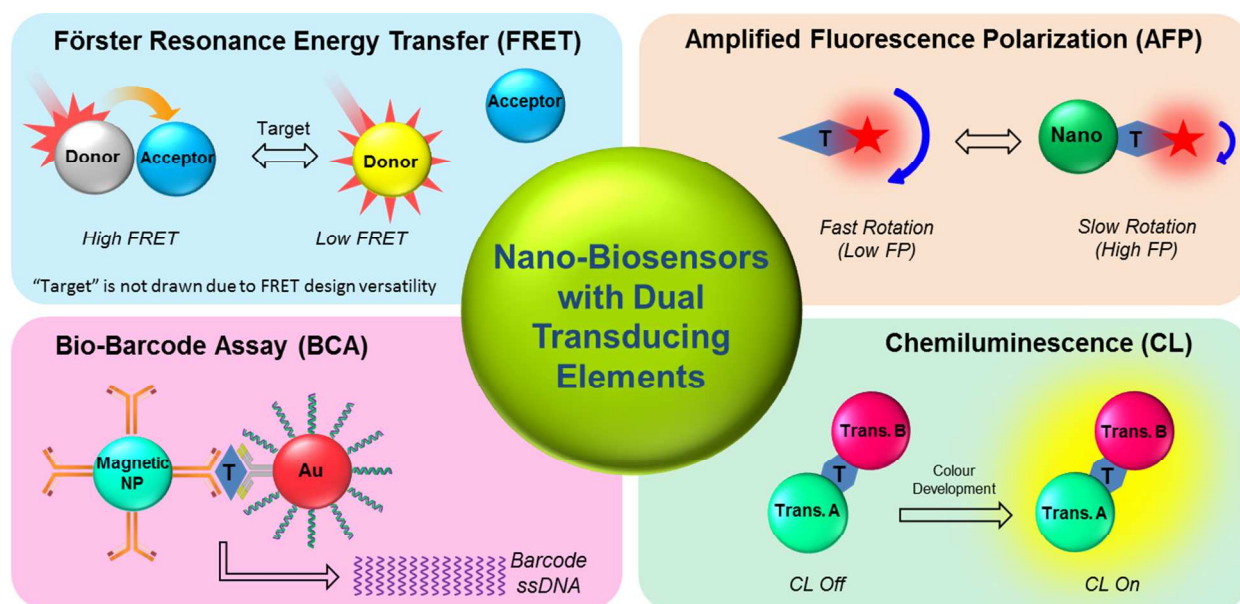


Yi Lu received his BS degree from Peking University in 1986, and a PhD degree from University of California at Los Angeles in 1992. After 2 years of postdoctoral research in Professor Harry B. Gray's group at Caltech, he started independent career in the Department of Chemistry at the University of Illinois at Urbana Champaign in 1994. He is now a Jay and Ann Schenck Professor of Chemistry in the Departments of Chemistry, Biochemistry, Bioengineering and Materials Science and Engineering. His research interests lie at the interface between chemistry and biology, including bioinorganic chemistry, biomaterials chemistry and bioanalytical chemistry.

Nanomaterial-based Biosensors using Dual Transducing Elements for Solution Phase Detection

Ning Li^a, Xiaodi Su^{a*}, Yi Lu^{a,b*}

TOC Entry



This review describes the design principles and recent advances of dual-transducer nanosensors ("T" = target; "Trans." in CL = Transducer)